JAERI-M
87-120

DEVELOPMENT OF TOKAMAK REACTOR CONCEPTUAL DESIGN CODE "TRESCODE"

—CONCEPTUAL DESIGN STUDY OF FY86 FER—

August 1987

Tadanori MIZOGUCHI*, Masayoshi SUGIHARA, Kichiro SHINYA**
Takeshi KOBAYASHI, Nobuharu MIKI, Kunihiko NAKASHIMA
Ryusei SAITO, Masao YAMADA, Noboru FUJISAWA
Shin YAMAMOTO, Hiromasa IIDA, Satoshi NISHIO and
FER Design Team

日本原子力研究所
Japan Atomic Energy Research Institute

JAERI-M レポートは，日本原子力研究所が不定期に公刊している研究報告書です。
入手の問合わせは，日本原子力研究所技術情報部情報資料課（〒319—11 茨城県那珂郡東海村）あて，お申しこしください。なお，このほかに財団法人原子力弘済会資料センター（〒319-11 茨城県那珂郡東海村日本原子力研究所内）で複写による実費頒布をおこなっております。

JAERI-M reports are issued irregularly.
Inquiries about availability of the reports should be addressed to Information Division, Department of Technical Information, Japan Atomic Energy Research Institute, Tokai-mura, Naka-gun, Ibaraki-ken 319-11, Japan.

編集兼発行　日本原子力研究所
印　　刷　山田軽印刷所

JAERI-M 87-120

Development of Tokamak Reactor Conceptual Design Code "TRESCODE"

— Conceptual Design Study of FY86 FER —

Tadanori MIZOGUCHI*, Masayoshi SUGIHARA, Kichiro SHINYA**
Takeshi KOBAYASHI, Nobuharu MIKI, Kunihiko NAKASHIMA
Ryusei SAITO, Masao YAMADA, Noboru FUJISAWA, Shin YAMAMOTO
Hiromasa IIDA, Satoshi NISHIO and FER Design Team

Department of Large Tokamak Research
Naka Fusion Research Establishment
Japan Atomic Energy Research Institute
Naka-machi, Naka-gun, Ibaraki-ken

(Received July 21, 1987)

Tokamak reactor system conceptual design code (TRESCODE) is developed on the basis of FER design studies. The code can be applied to the scoping studies for various reactor concepts. In this objects, relative cost estimations in terms of volume/weight and input/output energy can be carried out under the design driver/constraints of physics and engineering. Cost effective reactor concept is to be selected in this process. The code can also be used for engineering design of takamak core structure for the selected reactor concept. In this objects, accurate radial-build and vertical-build based on shield calculation and stress/strain analysis of magnet system can be carried out under the design constraints/conditions. Operation scenario is included with plasma equilibrium and poloidal field calculations to obtain the desired reactor concept.

Keywords : Tokamak, Conceptual Design, System Code, TRESCODE, FER

---

* On leave from Hitachi Ltd.

** Toshiba Corporation

[FER Design Team]

H. Iida, R. Saito, J. Adachi, K. Nakahara, H. Kuroda, S. Kashihara
S. Itoh, T. Nakayama, T. Suzuki, Y. Imamura, I. Nakazawa, T. Honda
H. Ohmura, T. Kobayashi, M. Yamada, T. Mizoguchi, S. Mori, J. Ohmori
Y. Imura, J. Sagawa, K. Maki, T. Watanabe, K. Sato, T. Kuroda
S. Yamazaki, A. Kameari, F. Matsuoka, S. Tado, K. Kitamura, T. Uchida
N. Miki, S. Suzuki, T. Hashizume, M. Konno, K. Toyoda, Y. Wachi
F. Iida, K. Nakashima, T. Uede, Y. Ishigaki, K. Miyamoto, M. Yamane
A. Ozaki, K. Okano, N. Fujisawa, S. Yamamoto, M. Sugihara, S. Hitoki
T. Okazaki, M. Abe, M. Kasai, N. Ueda, K. Shinya and A. Hatayama

JAERI－M 87－120

トカマク核融合炉概念設計コード"TRESCOD"の開発
－次期大型装置設計（FY86 FER）－

日本原子力研究所那珂研究所臨界プラズマ研究部
溝口忠憲*・杉原正芳・新谷吉郎**・小林武司・三木信晴
中島国彦・斉藤龍生・山田政男・藤沢　登・山本　新
飯田浩正・西尾　　敏・FER設計チーム

（1987年7月21日受理）

FERの設計研究に基づいてトカマク炉概念設計コード（TRESCODE）が開発された。このコードはいろいろな炉概念の概念検討に用いることができる。この目的のために，炉の体積／重量や入／出力エネルギーを用いて，物理か工学の設計条件の下に相対コストを算出することが可能である。これにより，性能－コスト比の高い炉を選定することができる。このコードはまた選定された炉概念に対して炉心構造の概略設計をすることができる。この目的のために，正確なラジアル／バーティカルビルドを，しゃへい計算やコイルの応力評価に基づいて計算する。プラズマ平衡とポロイダルコイル系の計算をコード内で行い，それに基づいて運転シナリオを検討することも可能である。

那珂研究所：〒311－02　茨城県那珂郡那珂町大字向山801－1
＊　外来研究員　㈱日立製作所
＊＊　㈱東芝

〔FER設計チーム〕

飯田　浩正・斉藤　龍生・安達　潤一・中原　克彦・黒田　秀夫・柏原晋一郎・伊東　新一
中山　尚英・鈴木　達志・今村　豊・中沢　一郎・本多　力・大村　博志・小林　武司
山田　政男・溝口　忠憲・森　清治・大森　順次・井村　泰也・佐川　準基・真木　紘一
渡辺　隆・佐藤　瓊介・黒田　敏公・山崎誠一郎・亀有　昭久・松岡　不識・田戸　茂
喜多村和憲・内田　孝穂・三木　信晴・鈴木　昌平・橋爪　隆・今野　雅行・豊田　勝義
和智　良裕・中島　国彦・藤沢　登・山本　新・杉原　正芳・一木　繁久・上出　泰生
石垣　幸雄・宮元　和弘・山根　実・尾崎　章・岡野　邦彦・岡崎　隆司・阿部　充志
笠井　雅夫・上田　憲照・新谷　吉郎・畑山　明聖

Contents

目　　次

1. Introduction

The tokamak reactor system conceptual design code (TRESCODE) has been developed at JAERI on the basis of FER design studies. There are two objects for developing the design code. The first object is that TRESCODE can be applied to the parameteric studies for various reactor concepts. In this objects, relative cost estimations in terms of volume/weight and input/output energy can be carried out under the design driver/constraints of physics and engineering. Cost effective reactor concept is to be selected in this process, while optimization will be desired for further studies. The second object is that TRESOCDE can be used for engineering design of tokamak core structure for the selected reactor concept. In this object, accurate radial-build and vertical-build based on the shield calculation and stress/strain analysis of magnet system can be carried out under the design constraints/conditions. Operation scenario is consistent with plasma equilibrium and poloidal magnetic field calculations to obtain the desired reactor concept.

The code consists of six major blocks, namely, plasma power balance calculation with core structure restriction, toroidal field coil design, poloidal field coil design with plasma equilibrium and field calculations, operation scenario, electric power supply analysis and relative cost estimation. Basic flow chart is shown in Fig. 1. In the process of determining the inner torus radial build, shield requirements given as constraints for neutron wall load and lifetime fluence are solved consistently by introducing a simplified shield calculation model. The radius of solenoid coils is also solved consistently under the necessary volt second required from burn time and operation scenario as the design driver. The current density of TFC's conductor is principally determined by the B-J_C relation. TFC case is designed to satisfy allowable stress intensity for primary membrane stress against in-plane and overturning force at all. Poloidal field coils' positions are automatically determined with reflecting prohibition regions such as access ports, torus core supporting legs, et. al.. PFC cross section and their final positions are solved consistently with the conductor design constraints and operation scenario. Operation scenario is one of important design driver to determine not only reactor size but also reactor's capability. In this code, however, one aspect of operation scenario, that is, a

required volt second is discussed in detail, because the reactor size and PFC system strongly depends on this considerations. The electric power supply is also estimated consistently with the operation scenario. The accumulated capacity of the power supplies for PFC will be dominant to compare with that for TFC. Our main considerations in this code is appropriate evaluation of the power supplies for PFC. In addition, the power supplies for heating and current driving is also discussed. Finally, cost estimation in terms of weight and energy is provided.

2. Plasma power balance

2.1 Basic equations

The simplified point-model power balance equations are used to obtain the plasma and device parameters, namely,

$$P_{con} + P_{br} + P_{sy} = P_{\alpha}(1 + \frac{5}{Q}) \tag{2.1}$$

where,

$$P_{con} = \frac{3}{2} kT \left(\frac{n_e}{\tau_{Ee}} + \frac{n_i}{\tau_{Ei}}\right) \quad \text{or} \tag{2.2}$$

$$\frac{\frac{3}{2} k (n_e + n_i) T}{\tau_E^{global}}$$

$$P_{br} = 1.41 \times 10^{-38} Z_{eff} n_e^2 \sqrt{T} \tag{2.3}$$

$$P_{sy} = 6.38 \times 10^{-16} B_T^{2.5} T^2 \sqrt{n_e/R} \tag{2.4}$$

$$P_{\alpha} = n_D n_T \langle\sigma v\rangle E_{\alpha} f_r \ . \tag{2.5}$$

All variables are in MKSA unit except for temperature (eV). n_e, n_i and T are the averaged electron density, ion density and plasma temperature assuming $T_e = T_i$, respectively. f_r is the numerical factor which represents the profile effect of density and temperature on fusion power. Q is the energy multiplication factor defined by P_{fusion}/P_{in}. E_{α} and $\langle\sigma v\rangle$ are α-particle energy produced by DT fusion reaction and its reaction rate. We use the following functional form for $\langle\sigma v\rangle$,

$$\langle\sigma v\rangle = 1.0 \times 10^{-22} \exp[0.038245 (\ln T_{kev})^3 - 1.0074 (\ln T_{kev}) + 6.3977 (\ln T_{kev}) - 9.75] \tag{2.6}$$

where $T_{kev} = T/10^3$ (keV).

2.2 Energy confinement

τ_{Ee}, τ_{Ei} and τ_E^{global} in Eq. (2.2) are the electron energy confinement time, ion energy confinement time and global energy confinement time, respectively. Various confinement time scalings are incorporated in the code as follows.

$$\tau_E^{Mirnov}{}^{(1)} = 0.155 \times 10^{-6}\ a\ I_p\ \sqrt{\kappa} \tag{2.7}$$

$$\tau_E^{Optimized}{}^{(2)} = 0.046\ R\ a\ B_T\ \sqrt{M} \tag{2.8}$$

$$\tau_E^{INTOR/Alcator}{}^{(3)} = 5.0 \times 10^{-21}\ n_e\ \kappa\ a^2 \tag{2.9}$$

$$\tau_E^{neo\text{-}Alcator}{}^{(4)} = 7.0 \times 10^{-22}\ n_e\ a\ R^2\ \sqrt{q_\psi} \tag{2.10}$$

$$\tau_E^{ASDEX\text{-}H}{}^{(5)} = 0.064 \times 10^{-6}\ R\ I_p\ \sqrt{M} \tag{2.11}$$

$$\tau_E^{T\text{-}11}{}^{(6)} = 0.014 \times 10^{-20}\ n_e\ a^{0.25}\ R^{2.75}\ \sqrt{M}/\sqrt{T} \tag{2.12}$$

$$\tau_E^{Goldston}{}^{(7)} = 0.023 \times 10^{-3}\ I_p\ \kappa^{0.5}\ a^{0.37}\ R^{1.75}\ \sqrt{M}/\sqrt{P_{in}} \tag{2.13}$$

where I_p is plasma current, κ plasma elongation, M ion mass, q_ψ safety factor at edge, and P_{in} input power. Mirnov type scaling is used as a reference for the FER design.

2.3 Beta limit and fuel density

Several models for beta limit are incorporated in the code as follows.

Troyon scaling[8]:
$$\beta_c^{Troyon}(\%) = G\ \frac{I_p(MA)}{aB_T} \tag{2.14}$$

JAERI scaling[9]:
$$\beta_c^{JAERI}(\%) = \frac{30\ \kappa^{1.5}}{A\ q_\psi}\left\{1.0 + 0.9(\kappa-1)\delta - 0.6\ \frac{\kappa^{0.75}}{q_\psi} + 14(\kappa-1)(1.85-\kappa)\ \frac{\delta^{1.5}}{q_\psi^4}\right\} \tag{2.15}$$

GA scaling[10]:
$$\beta_c^{GA}(\%) = C\ \varepsilon^{1.3}\ \kappa^{1.2}(1+1.5\delta)q_\psi^{-1.1} \tag{2.16}$$

$$\text{Yamazaki scaling}^{(11)}: \quad \beta^{\text{Yamazaki}}(\%) = \frac{4.7\ I_p(\text{MA})}{aB_T}\left\{1 - b\ \frac{I_p(\text{MA})}{aB_T}\right\} \tag{2.17}$$

$$b = 0.065\ \frac{A}{\sqrt{\kappa}}\left\{1 - \frac{\kappa-1+0.05\delta}{\sqrt{\kappa}} \times \left(\frac{1+1.5\delta}{\kappa}\right)^{2.5}\right\} \tag{2.18}$$

where A and ε are the aspect ratio and inverse aspect ratio, respectively. δ is plasma triangularity. Troyon scaling is used as a reference for FER design and Yamazaki scaling may be used for the option design of extremely shaped tokamaks.

JAERI model is also prepared for the relation between q_ψ and I_p being consistent with MHD analysis,

$$q_\psi^{-1} = \sqrt{1 - 1/A^2}\ \left(\frac{2}{1+\kappa^2} - 0.08\delta\right)\frac{\mu_0 A I_p}{2\pi a B_T} - 0.07\{1 + (\kappa-1)\delta\} \tag{2.19}$$

We also use the emperical expression[12] based on equilibrium calculations such as

$$q_\psi = \frac{2\pi}{\mu_0}\frac{aB_T}{AI_p}\frac{1+\kappa^2}{2}\left(1 + \frac{0.16+0.633\delta}{\sqrt{A}}\right)\left\{1 + \frac{\beta_p(0.45+\delta)}{A^{1.5}}\right\} \tag{2.20}$$

where β_p is poloidal beta.

Although the total α density could reach the order of the background density, some fraction of fast α particles not in losing during their slowing down would contribute to the total pressure. The ratio Γ_α of fast α pressure to background plasma pressure has a strong dependence on background plasma temperature. According to Jassby's studies[13], Γ_α may be approximated by the following form.

$$\begin{aligned} \Gamma_\alpha &= 0 && (T \le 7\ \text{keV}) \\ &= 0.015\ T_{\text{keV}} - 0.1 && (7\ \text{keV} \le T \le 30\ \text{keV}) \end{aligned} \tag{2.21}$$

Improvement of this expression by using the steady state solution of Fokker-Planck equation is now under way.

Including the helium ash concentration and some impurities, fuel densities, n_D and n_T, are given as

$$n_D = \frac{1}{4.03\times10^{25}} \frac{f_D}{1+f_{ei}} \frac{\beta_C}{1+\Gamma_\alpha} \frac{B_T^2}{T} \tag{2.22}$$

$$n_T = \frac{1}{4.03\times10^{25}} \frac{f_T}{1+f_{ei}} \frac{\beta_c}{1+\Gamma_\alpha} \frac{B_T^2}{T} \tag{2.23}$$

where f_D and f_T are the ratio of deutron and tritium density to total ion density n_i, f_{ei} is the ratio of total electron density to total ion density. These are input parameters in the code and typical values in the FER design are $f_D = f_T = 0.465$, f_{He} (helium) = 0.05, f_H(hydrogen isotope) = 0.01, f_C (carbon) = 0.005 and f_{ox} (oxygen) = 0.005 so that $f_{ei} \simeq 1.11$ and $Z_{eff} \simeq 1.5$.

2.4 Plasma heating and current drive powers

Plasma heating power density, P_{heat}, is determined by solving the following power balance equations,

$$P_{con} + P_{br} + P_{sy} = P_\alpha + P_J + P_{heat} \tag{2.24}$$

where P_J is the joule heating power density. We assume two heating passes, namely

$$\text{Pass 1;} \quad n(T) = \text{const.} \tag{2.25}$$

$$\text{Pass 2;} \quad n(T) = \frac{n_e - n_{ig.app.}}{T_B} T \tag{2.26}$$

where n_e is the electron density of the ignition plasma, $n_{ig.app}$ is the electron density at the begining of ignition approach phase, assuming $\sim 3 \times 10^{18}$ m^{-3}, and T_B is burning plasma temperature at operation point. Plasma heating power P_H is then given by

$$P_H = \text{Max.}[P_{heat}(\text{Pass 1}), P_{heat}(\text{Pass 2})] \times \text{Vol} \times \text{SF} \tag{2.27}$$

where Vol is the plasma volume, $2\pi^2\kappa a^2 R_p$, and SF is a marginal safety factor.

Current drive power is estimated from a current drive efficiency η_{drive}.

(i) Case of NBI current drive

Current drive power P_{CD}^{NBI} is given by[14]

$$P_{CD}^{NBI} = \frac{I_P}{\eta_{NBI}} \tag{2.28}$$

where

$$\eta_{drive}^{NBI} \simeq A_{bd} \frac{5}{R_p}(1-f_s)\frac{R_{tang}}{R_p}\frac{<T_e>_{10}}{<n_e>_{20}}\frac{0.2\ J(x',y)}{0.2}F(Z_b,Z_{eff},\frac{a}{R_p}) \tag{2.29}$$

A_{bd}: coefficient for current drive efficiency (~0.11 A/Watt)

$$f_s = e^{-\tau} \tag{2.30}$$

$$\tau = 1.7\ n_e\ \sigma_{eff}\ R_p \tag{2.31}$$

$$\sigma_{eff} \simeq \frac{1}{2.8 \times 10^{13}\ E_b\ (keV)} \tag{2.32}$$

E_b (keV): beam energy

$$R_{tang} = R_p - \frac{a}{s} \tag{2.33}$$

$$J(x',y) = x'^2/[A+3y+X'^2(x'+1.39+0.61\ y^{0.7})] \tag{2.34}$$

$$x' = \sqrt{\frac{E_b}{B_{bd}E_c}} \tag{2.35}$$

$$B_{bd} = 2.0 \tag{2.36}$$

$$E_c \simeq 100(keV)\ A_b <T>_{10} \tag{2.37}$$

A_b = beam mass

$$y = \frac{Z_{eff}}{5A_b} \tag{2.38}$$

$$<n_e>_{20} = n_e/10^{20} \tag{2.39}$$

$$<T>_{10} = T/10^4 \tag{2.40}$$

$$F(Z_b,Z_{eff},\varepsilon) = \frac{1}{Z_b} - \frac{1}{Z_{eff}}\ [1 - G(Z_{eff},\ \varepsilon)] \tag{2.41}$$

Z_b: Atomic number of beam

$$G(Z_{eff},\ \varepsilon) \simeq (1.55+\frac{0.85}{Z_{eff}})\sqrt{\varepsilon} - (0.20+\frac{1.55}{Z_{eff}})\varepsilon \tag{2.42}$$

A_{bd}, E_b, Z_b, A_b and S are input in the code. $<n_e>_{20}$ and $<T>_{10}$ are specified by operation scenario.

3. Inner torus radial-build and shield requirements

3.1 Inner torus radial-build

Schematic radial-build of tokamak system is shown in Fig. 2. If a necessary volt second $\Delta\phi$ is given by the operation scenario, the outer radius of solenoid coils, R_{sol}, is evaluated by the following equations.

$$\Delta\phi = 2B_{Pmax}(1 - f_{EQ}) \times \pi(R_{sol}^2 - R_{sol}\cdot\Delta_P + \frac{\Delta_P^2}{3}) \tag{3.1}$$

$$B_{Pmax} = \alpha_p \gamma f_{PS} \mu_0 J_{pw} \Delta_P \tag{3.2}$$

where B_{Pmax} and J_{pw} are allowable maximum field and maximum current density of the solenoid coils, respectively, which are specified as design conditions. γ is a correction coefficient for the finiteness of the solenoid coils. f_{PS} is a space occupation ratio of the superconductor over the solenoid coils including support structures. α_p is the ripple correction factor for the descreteness in Z direction. f_{EQ} represent a fraction of field reduction due to divertor coil field on hybrid-type solenoid coils. f_{EQ} strongly depends on plasma shape and operation scenarios. In the code, f_{EQ} is initially given but exact R_{sol} is evaluated by iterative method described in Sec. 7.

Toroidal field coil's thickness is calculated from the following equation,

$$\frac{B_{Tmax}}{\alpha_T} = \frac{\mu_0 J_{tw}\cdot 2\pi f_{ts}(R_T + \frac{\Delta_T}{2})\Delta_T}{2\pi (R_T + \Delta_T)} \tag{3.3}$$

$$R_T = R_{sol} + \Delta_{gap} + \Delta_{BC} + \Delta_{can1} \tag{3.4}$$

where B_{Tmax} and J_{tw} are allowable maximum field and current density, respectively, which are specified as design conditions. f_{ts} is the space factor of conductor in the toroidal direction. α_T is the ripple correction factor due to the discreteness at the inner leg. Δ_{gap} is specified. Δ_{BC}, Δ_{can1} and Δ_{can2} are initially given.

Thermal shield thickness Δ_{TS} and vaccum vessel thickness Δ_{VV} are specified. Initial values of shield thickness Δ_{SDI} and blanket/shield thickness Δ_{BLI} are given. Finally plasma scrape-off thickness of inner

torus Δ_{SOI} is specified from impurity control requirement, then the distance Δ between TFC and inner plasma edge is given by

$$\Delta = \Delta_{can2} + \Delta_{TS} + \Delta_{VV} + \Delta_{SDI} + \Delta_{BLI} + \Delta_{SDI} \ . \tag{3.5}$$

As a result, toroidal field at plasma center B_T is given as

$$B_T = \frac{B_{Tmax}}{\alpha} \left(1 - \frac{a+\Delta}{R}\right) \tag{3.6}$$

Under the restrictions of inner torus radial-build given by Eqs. (3.1), (3.2), (3.3), (3.4) and (3.5), plasma power balance equation, Eq. (2.1) can be solved with Eq. (3.6).

3.2 Shield requirements

Neutron wall load is determined from the above process. Here, the shield thickness is reexamined whether it is enough for a given lifetime fluence and wall load. Effective shield thickness Δ_{eff} is

$$\Delta_{eff} = f_{BLI}\ \Delta_{BLI} + f_{SDI}\ \Delta_{SDI} + f_{VV}\ \Delta_{VV} + f_{can2}\ \Delta_{can2} \ (cm) \tag{3.7}$$

f_{BLI} : Effective thickness factor for blanket

f_{SDI} : Effective thickness factor for shield

f_{VV} : Effective thickness factor for vacuum vessel

f_{can2} : Effective thickness factor for helium can

Note : For effective thickness factors,
$f_{BLI} = f_{SDI} = f_{VV} = f_{can2} \simeq 0.9$ is assumed in the current calculation.

Shielding responses are calculated approximately by the following equation:

$$R(i) = T(i) P_w(Mw/m^2) R_{FW}(i)\ e^{-\mu_s(i)\Delta_{eff}(i)} \tag{3.8}$$

R(1) : Nuclear heating rate of SC (W/cm^3)

R(2) : Copper atomic displacement (dpa)

R(3) : Insulator absorbed dose (rad)

R(4) : Fast neutron fluence (cm^{-2})

$R_{FW}(i)$: Response at first wall

$\mu_s(i)$: Effective attenuation coefficient (cm^{-1})

T(i) : Total irradiation period during lifetime (sec) (except T(1)=1)

These factors are summarized in the following table based on the design of FER(FY1986):

i	$R_{Fw}(i)$	$\mu_s(i)$ (a)
1	10.3 (W/cm^3) (b)	0.1302
2	3.33×10^{-7} (dpa/s)	0.1431
3	7.08×10^{5} (rad/s)	0.1383
4	2.19×10^{14} $(I/cm^2/s)$	0.1324

(a) Shield composition: SS316-85%, H_2O-15%

(b) SC composition : SS316-34%, Cu-33%

On the other hand, total nuclear heating is estimated by the following;

i) Nuclear heating in front wall of helium can (neglect nuclear heating in rear wall)

Nuclear heating in the front wall of the helium can is calculated by the following equation:

$$h_{can} = 2\pi(r_c + \Delta_{can2})(1 - f_{ts})\ell\, h_c \int_0^{\Delta_{can2}+\Delta_T} e^{-\mu_c t}\, dt \qquad (3.9)$$

$$+ 2\pi(r_c + \Delta_{can2}) f_{ts}\, \ell\, h_c \int_0^{\Delta_{can2}} e^{-\mu_c t}\, dt$$

where,

f_{ts} : Space factor of TFC conductor in toroidal direction

h_c : $P_w R_{FW}(1) e^{-\mu_s(1)(\Delta_{eff} - f_{can2}\Delta_{can2})}$ (3.10)

ℓ : Poloidal length of TFC in the inboard part of the torus which dominates total nuclear heating (see the note)

$f_c = R - a - \Delta$

h_c : Nuclear heating rate at the front surface of helium can

h_m : Nuclear heating rate at the front surface of superconductor

ii) Nuclear heating in superconductor

Nuclear heating in the superconductor is calculated by the following equation:

$$h_{sc} = 2\pi r_c f_{ts} \ell h_m \int_0^{\Delta_T} e^{-\mu_{SCM} t} dt \tag{3.11}$$

$$h_m = P_W R_{FW} R_{FW}(1) e^{-\mu_s(1)\Delta_{eff}} \tag{3.12}$$

iii) Total nuclear heating in TFC

Total nuclear heating in TFC, R(5), is therefore, calculated as follows:

$$\begin{aligned} R(5) &= h_{can} + h_{sc} \\ &= 2(r_e+\Delta_{can2})\ell h_c \left[(1-f_{ts}) \int_0^{\Delta_{can2}+\Delta_T} e^{-\mu_c t} dt \right. \\ &\quad \left. + f_{ts} \int_0^{\Delta_{can2}} e^{-\mu_c t} dt \right] + 2\pi r_c \ell h_m \int_0^{\Delta_T} e^{-\mu_{sc}} dt \\ &\equiv E_c h_c + E_m h_m \end{aligned} \tag{3.13}$$

where, attenuation coefficients for nuclear heating rate, μ_c, μ_{sc} are given in the following table:

μ_c	0.1066 (Δ_{eff} = 65 cm)
μ_{sc}	0.1976 (Δ_{eff} = 76.6 cm)

Attenuation coefficient, μ_{sc} is correlated to the effective shield thickness, Δ_{eff} by the following relationship:

$$\mu_{sc} = 0.0078\ \Delta_{eff} - 0.403$$

<Note> Determination of the dominant poloidal length of TFC, l

The dominant poloidal length of TFC in the inboard part of the torus, l is assumed to be equal to the plasma height:

For SND, $\ell = \kappa_u a + \kappa_N a$

For DND, $\ell = 2 \times \kappa_N a$

After all, Required effective shield thickness is calculated by the following equation:

$$\Delta_{eff}(i) = -\frac{1}{\mu_s(i)} \ln\left[\frac{R^D(i)}{T(i)\ P_w\ R_{FW}(i)}\right] \quad (i = 1 \sim 4) \tag{3.14}$$

$$\Delta_{eff}(5) = -\frac{1}{\mu_s(1)} \ln\left[\frac{R^D(5)}{(E_c+E_m)\ P_w\ R_{FW}(1)}\right] \tag{3.15}$$

Maximum of $\Delta_{eff}(i)$ is a necessary effective shield thickness. If the initial value of Δ_{eff} is thiner or thicker than maximum $\Delta_{eff}(i)$, Δ_{eff} is adjusted and the power balance equation is solved iteretively until appropriate shield thickness is obtained.

Finally, shielding design criteria are summarized in the following table:

	Design Criteria
$R^D(1)$	1×10^{-3} w/cm^3
$R^D(2)$	4×10^{-4} dpa
$R^D(3)$	3×10^9 rad
$R^D(4)$	2×10^{18} cm^{-2}
$R^D(5)$	15 kW
Fluence	0.3 MW·Y/m^2

As copper atomic displacement damage can be recovered by the room temperature annealing, the copper dpa criterion, $R^D(2)$ is not applied strictly.

Total irradiation period is calculated based on the lifetime fluence as follows:

$$T(i) = \text{fluence} \times 365 \times 24 \times 60 \times 60 \; / \; P_w$$

$$= 3.154 \times 10^7 \times \text{fluence} \; / \; P_w \; (\text{sec})$$

4. Toroidal field coil design

4.1 Conductor design

Design of cable-in-conduit type forced flow superconductor carried out by the following process;

(1) Constraints of TFC conductor design.

i) Winding current density $j_{pack} \leq 35$ A/mm^2

ii) Maximum field of conductor $B_m \leq 12$ T

iii) Superconducting material is $(Nb \cdot Ti)_3S_n$

iv) Operating current I_{op} ~30 KA

v) Maximum terminal voltage $V_{max} \leq 20$ kV

vi) Maximum pressure in the conduit $P_{max} \leq 15$ MPa

vii) Using cable-in-conduit type forced flow superconductor.

viii) Coil manufacturing process is Wind and React.

(Maximum allowable Strain of winding is 6×10^{-3}.)

(2) Other conditions

i) Void area fraction $f_{co} = 0.4$

ii) Maximum hot spot temperature $T_{max} = 100$ K

iii) Conduit area fraction $1 - f_w = 0.4$

iv) Temperature margin $T_{cs} - T_b = 2$ K

(3) Design process of TFC superconductor

The current density of the conductor J[A/mm^2] is calculated using following formulas;

$$J = 18.66\, R_m^2\, f^2 \qquad (4.1)\ \text{[strain limit of winding]}$$

$$= 0.36 J_c (1 - f) \Delta T \qquad (4.2)\ \text{[temperature margin limit]}$$

$$= 50.2 \frac{f^{\frac{1}{2}}}{d} \sqrt{\frac{\Delta T}{\rho}} \qquad (4.3)\ \text{[limiting current condition]}$$

$$\Delta T = 18.3 \left(1 - \frac{B_m}{24.5}\right)^{\frac{1}{2}} - 5 \qquad (4.4)\ \text{[temperature margin]}$$

$$J_c = 2300 \left(1 - \frac{B_m}{24.5}\right)^2 \ [A/mm^2] \qquad (4.5)\ \text{[critical current density]}$$

$$\rho = 0.63 + 0.48 B_m \ [\times 10^{-10}\ \Omega \cdot m] \qquad (4.6)\ \text{[electric resistivity of stabilizer]}$$

The stabilizer area fraction f is calculated from following formula;

$$f = \frac{\sqrt{0.0324 J_c^2 \Delta T^2 + 6.72 R_m^2 J_c \Delta T} - 0.18 J_c \Delta T}{18.66 R_m^2} \qquad (4.7)$$

The strand diameter d is calculated from following formula;

$$d = \frac{2.69}{R_m^2 f^{\frac{3}{2}}} \sqrt{\frac{\Delta T}{\rho}} \tag{4.8}$$

4.2 Determination of TFC shape and its characteristics

Position of TFC inner leg defined at the center of the conductor, R_1, is determined by the inner torus radial-build constraints. On the other hand, position of outer leg, R_2, will be determined by a constraint of toroidal field ripple δ at plasma edge, $R_p + a$, namely,

$$R_2 = \left[\left\{ \frac{c\,\delta\,N}{21} - \frac{1}{\left(\frac{R_p + a}{R_1}\right)^N - 1} \right\}^{-1} + 1 \right]^{\frac{1}{N}} (R_p + a) \tag{4.9}$$

where N is a number of TF coils and c is a correction coefficient.

By following the Princeton-D type coil shape[16], the height of TFC bore h_Z^{CT} is given by

$$h_Z^{CT} = \pi\, r_0\, k \left[I_1(k) + L_1(k) + \frac{2}{\pi} \right] \tag{4.10}$$

where

$$r_0 = \sqrt{R_1 R_2} \tag{4.11}$$

$$k = \frac{1}{2} \ln \left(\frac{R_2}{R_1} \right) \tag{4.12}$$

I_n = modified Bessel function

L_1 = first order modified Struve function

Another characteristics for the Princeton D type coil such as the height of coil straight section at the inner leg, h_ℓ^{CT}, the perimeter, ℓ_t^{CT}, the coil area A_t^{CT}, and the inductance for a torus with N_t total turns, L^{CT}, are given as,

$$h_\ell^{CT} = 2\pi\, r_0\, k\, I_1(k) \tag{4.13}$$

$$\ell_t^{CT} = 2\pi\, r_0\, k[I_0(k) + I_1(k)] \tag{4.14}$$

$$A^{CT} = 2\pi\, r_0^2\, k[I_1(2k) - e^{-k} I_1(k)] \tag{4.15}$$

$$L^{CT} = \frac{\mu_0 \, r_0 \, N_t^2 \, k^2}{2} \left[I_0(k) + 2I_1(k) + I_2(k) \right] \tag{4.16}$$

The stored energy is

$$E_S^{CT} = \frac{1}{2} L \, I_{op}^2 \tag{4.17}$$

where I_{op} is the operational current

In case of the actual design, the height of TF coil h_z should be determined by the vertical-build constraints, that is,

for limiter configuration,

$$h_z = 2 \times (\kappa a + \Delta_{VSO} + \Delta_{VBL} + \Delta_{VSD} + \Delta_{VVV} + \Delta_{Vgap} + \frac{\Delta_T}{2}) \tag{4.18}$$

for single null divertor configuration,

$$h_z = \kappa_u \, a + \Delta_{VSO} + \Delta_{VBL} + \Delta_{VSD} + \Delta_{VVV} + \Delta_{Vgap} + \frac{\Delta_T}{2} + \kappa_N \, a + \Delta_{Div} + \Delta_{VBL} + \Delta_{VSD} + \Delta_{VVV} + \Delta_{Vgap} + \frac{\Delta_T}{2} \tag{4.19}$$

for double null divertor configuration,

$$h_z = 2 \times (\kappa_N \, a + \Delta_{DiV} + \Delta_{VBL} + \Delta_{VSD} + \Delta_{VVV} + \Delta_{Vgap} + \frac{\Delta_T}{2}) \tag{4.20}$$

where

Δ_{VSO} : scrape-off thickness of upper edge or bottom edge plasma

Δ_{VBL} : shield/blanket thickness at top and bottom

Δ_{VSD} : shield thickness at top and bottom

Δ_{VVV} : vaccum vessel thickness at top and bottom

Δ_{Vgap} : space between VV surface and inside He can of TFC

Δ_{Div} : divertor thickness defined as a distance between null point and bottom of divertor system

The difference of the TFC height between the Princeton D shape and the actual design shape, Δh_z, is given as $\Delta h_z = h_z^{CT} - h_z$.

The height of actual coil straight section is set by, for convenient sake,

$$h_{\ell} = h_{\ell}^{CT} - \Delta h_z \ . \tag{4.21}$$

Then, three points are defined as $A(R_1, h_{\ell}/2)$, $B(r_0, h_z/2)$ and $C(R_2, 0)$ on the upper half and TFC shape is determined by three-arc approxiamtions. The inductance of the actual coil is approximated by the following correction,

$$L \simeq \frac{A}{A^{CT}} \frac{\ell_t}{A_t^{CT}} L^{CT} \tag{4.22}$$

where A and ℓ_t are the coil area and perimeter of the actual designed coil, respectively. The above correction fits fairly well the results of three dimensional field calculation. The stored energy then is given by

$$E_S = \frac{1}{2} L I_{op}^2 \tag{4.23}$$

4.3 Stress analysis

(1) Stress calculations of coil case

By the three-arc approximation, the centers of each arc, (x_1, z_1) (x_2, z_2) and (x_3, z_3), their radii, A_1, A_2, A_3 and their angles θ_1, θ_2, θ_3, are determined automatically with giving either the first arc's angle θ_1 or the radius A_3. Then in-plane electromagnetic forces such as hoop force F_H, centering force F_R and vertical force F_Z are given as

$$F_H = 2\left[\int_0^{\theta_1} \frac{\mu_0 NI^2 \cdot A_1 \, d\theta}{4\pi(x_1 + A_1 \cos\theta)} + \int_{\theta_1}^{\theta_1+\theta_2} \frac{\mu_0 NI^2 \cdot A_2 \, d\theta}{4\pi(x_2 + A_2 \cos\theta)}\right.$$

$$\left. + \int_{\theta_1\ \theta_2}^{\pi} \frac{\mu_0 NI^2 \cdot A_3 \, d\theta}{4\pi(x_3 + A_3 \cos\theta)}\right] + \frac{\mu_0 NI^2}{4\pi R_1} \times h_z \tag{4.24}$$

$$F_R = 2\left[\int_0^{\theta_1} \frac{\mu_0\, NI^2 \cdot A_1 \cos\theta\, d\theta}{4\pi(x_1 + A_1\cos\theta)} + \int_{\theta_1}^{\theta_1+\theta_2} \frac{\mu_0\, NI^2 \cdot A_2 \cos\theta\, d\theta}{4\pi(x_2 + A_2\cos\theta)}\right.$$

$$\left. + \int_{\theta_1+\theta_2}^{\pi} \frac{\mu_0\, NI^2 \cdot A_3 \cos\theta\, d\theta}{4\pi(x_3 + A_3\cos\theta)}\right] - \frac{\mu_0\, NI^2}{4\pi\, R_1} \times h_z \qquad (4.25)$$

$$F_Z = \int_0^{\theta_1} \frac{\mu_0\, NI^2 \cdot A_1 \sin\theta\, d\theta}{4\pi(x_1 + A_1\cos\theta)} + \int_{\theta_1}^{\theta_1+\theta_2} \frac{\mu_0\, NI^2 \cdot A_2 \sin\theta\, d\theta}{4\pi(x_2 + A_2\cos\theta)}$$

$$+ \int_{\theta_1+\theta_2}^{\pi} \frac{\mu_0\, NI^2 \cdot A_3 \sin\theta\, d\theta}{4\pi(x_3 + A_3\cos\theta)} \qquad (4.26)$$

where NI is the total ampere turns and N is the number of TF coils. The centering force and vertical force are also given in analytical form such as

$$F_R = 2\pi\left(R_1 + \frac{\Delta_T}{2}\right)\frac{B_{Tmax}^2}{2\mu_0\, N} \quad (N/m) \qquad (4.27)$$

$$F_Z = \frac{\mu_0\, NI^2}{4\pi}\, In\, \frac{R_2}{R_1} \quad (N) \qquad (4.28)$$

On the other hand, overturing force F_Y is given by

$$F_Y = B_{pn}^{int} \times \frac{NI}{N} \quad (N/m) \qquad (4.29)$$

where B_{pn}^{int} is the initial-guess value of the poloidal field normal to the current flow of TFC.

The following stresses occur in the coil case and the bucking cylinder.

(i) Outer ring

Tensile stress due to the tension force and bending stress due to the centering force at the upper and lower shoulders of inner leg.

(ii) Inner ring

Tensile stress due to the tension force and bending stress due to the out-of-plane force

(iii) Side plate

Tensile stress due to the tension force and bending stress due to the out-of-plane force

(iv) Bucking cylinder

Compressive stress due to the centering force

The principal stress of the coil case is shown below. The steel in the winding is not counted in the TF Coil stress calculation.

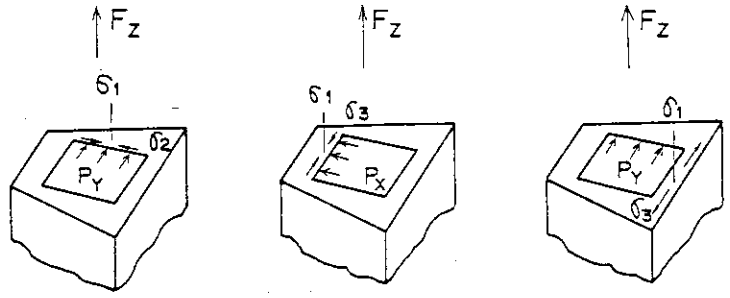

Side plate Outer ring Inner ring

The average inplane stress by inplane force is obtained by

$$\sigma_1 = K_0 \frac{F_z}{A_{can}} \qquad K_0 : \text{ factor (1.5 for FER)} \tag{4.30}$$

where A_{can} is the coil case cross sectional area. The bending stress of the outer ring by centering force and overturning force are given by the following, respectively,

$$\sigma_{31}(\text{outer ring}) = K_1 \frac{F_R}{b} \left(\frac{b}{\Delta_{can1}} \right)^2 \tag{4.31}$$

$$\sigma_{32}(\text{outer ring}) = K_2 \frac{F_Y}{2\,\Delta_{can1}} \left(1 + \frac{\Delta_{TF}}{4\,\Delta_{can1}}\right) \tag{4.32}$$

where

$$b = 2 f_{ts} R_1 \tan\frac{\pi}{N} \tag{4.33}$$

K_1: factor (0.5 in FER)

K_2: factor (0.75 in FER)

The bending stress of the inner ring by overturning force is given by

$$\sigma_3(\text{inner ring}) = \frac{K_3 F_y}{\Delta_{can2}} \left(1 + \frac{\Delta_{TF}}{8\,\Delta_{can2}}\right) \tag{4.34}$$

K_3: factor (0.5 in FER)

The bending stress of the side plate by overturning force is

$$\sigma_3(\text{side plate}) = \frac{K_4 F_Y \Delta_{TF}}{\Delta_{can3}^2} \tag{4.35}$$

where

$$\Delta_{can3} = R_1 \tan\frac{\pi}{N} - \frac{b}{2} \tag{4.36}$$

K_4: factor (0.91 in FER)

(2) Constraints on stress intensity

We use the following data for yield strength σ_y and tensile strength σ_u of coil case materials;

	SUS304LN	SUS316LN
σ_y	765.2 MPa	861.2 MPa
σ_u	1648.1 MPa	1378 MPa

Allowable stress intensity for primary membrane stress, S_m, is then given by

$$S_m = \text{Min.}\left\{\frac{2}{3}\sigma_y\ ,\ \frac{1}{3}\sigma_u\right\} \tag{4.37}$$

Constraints on stress intensity of TFC case is set by

$$\sigma_{a,i} = \frac{1.5 \times S_m}{SF_i} \tag{4.38}$$

where i = 1 represent the outer ring, i = 2 inner ring and i = 3 side plate. SF_i shows the safety factor. The coil case is determined to satisfy the following criteria;

for outer ring, $\sigma_1 + \sigma_{31} - \sigma_{32} \leq \sigma_{a1}$ (4.39)

for inner ring, $\sigma_3(\text{inner ring}) \leq \sigma_{a2}$ (4.40)

for side plate, $\sigma_1 + \sigma_3(\text{side plate}) \leq \sigma_{a3}$ (4.41)

However actual overturning force is not clear until PFC system design is carried out. When the poloidal field normal to the coil current flow, B_{pn}, obtained by field calculations after magnet system design is larger than the initial value B_{pn}^{int}, the above criteria Eqs. (4.39) through (4.41) are reexamined. If one criterion at least would be violated, side plate of the coil would be changed with adjusting the space factor f_{ts} and the whole calculations would be carried out

(3) Bucking cylinder

A bucking cyclinder is basically used for support system over centering force. Wedge support method is also considered for further studies. Average compressive stress of bucking cylinder is given by

$$\sigma_c(\text{bucking cylinder}) = \frac{N F_R}{2\pi \Delta_{BC}} \tag{4.42}$$

On the other hand, allowable stress of bucking cylinder is

$$\sigma_{a4} = \frac{S_m}{SF_4} \tag{4.43}$$

and allowable buckling stress of bucking cylinder is given by

$$\sigma_{ca}(\text{Bucking cylinder}) = \frac{E \times \Delta_{BC}^2}{12(1-\nu^2) \times R_{BC}^2} \tag{4.44}$$

$$R_{BC} = R_{sol} + \Delta_{gap} + \frac{\Delta_{BC}}{2} \tag{4.45}$$

where E is Young's modulus and ν is Poisson's ratio. Hence, the thickness of the bucking cylinder is determined to satisfy the following criteria,

$$\sigma_c \leq \text{Min}\ [\sigma_{a4},\ \sigma_{ca}]\ . \tag{4.46}$$

5. Solenoid coil design and PFC positioning

5.1 Conductor design of solenoid coils

In a present stage, we use the similar conductor to TFC conductor described in Sec. 4.1. Constraints of PF coils' design are the following;

(i) Maximum field of OH coil is 12 T.
(ii) Operating current is 40 kA.
(iii) Current density in conductor is 30 A/mm^2.
(iv) Maximum stress of conduit material is 600 MPa.
(v) Maximum terminal voltage is 20 kV.
(vi) Peak conductor temperature at dump mode is 100 K.
(vii) Superconducting material is Nb_3Sn.
(viii) Coil manufacturing process is "Wind and React".

Figure 3 shows the relation of the OH coil radius and the allowable winding-pack current density as a function of total volt-seconds. Based on the total volt-seconds of 50 Vs, the proposed winding-pack current densities are about 28 A/mm^2 shown in Fig. 3.

5.2 Design of solenoid coil

The end radius R_{sol} and conductor thickness Δ_p of solenoid coils are determined by Eqs. (3.1) and (3.2). The height of one turn solenoid plus spport structure is set to one meter. Since the space ratio of conductors in solenoid coils is given as f_{ps} , cross section of one turn solenoid is given by $\Delta_p \times (f_s \times 1m)$.

Here the coil is designed to be self-supporting for the hoop forces. Namely the cross sectional area of the stainless steel conduit is chosen assuming that each turn in the OH coil would be locally self-supporting. Tensile stress of conduit materials by hoop force is then calculated by

$$\sigma = \frac{B_{Pmax}\, j_p \cdot (R_{sol} - \Delta_P)}{f} \tag{5.1}$$

$$f = \frac{\text{conduit area}}{\text{conductor area}} \tag{5.2}$$

5.3 Prohibition area on PFC positioning

In positioning of PF coils, prohibition regions are set by the following;

i) not interfere to TFC case

ii) not interfere to access port

iii) not interfere to torus support/exhaust duct

iv) not interfere to guard limiter.

The prohibition region (i) is defined by the following: TFC shape is given by three-arc approximation discribed in Sec. 4.3, the radii of which are A_1, A_2 and A_3. We set the contour along TFC shape, the radii of which are given by $A_1 + D$, $A_2 + D$, $A_3 + D$ and $D = \frac{\Delta_{TF}}{2} + \Delta_{canl} + \Delta_{hg}$ where Δ_{hg} is a clearance gap. Then inside contour is defined as the prohibition area for (i). Another prohibition regions are defined on the X-Z coordinates. For instance, the prohibition region (ii) for the horizontal access port is defined by

$$Z_{bottom} \leq Z_H \leq Z_{top} \tag{5.3}$$

$$R_p \leq X_H \tag{5.4}$$

where, for single null

$$Z_{bottom} = Z_P - \kappa_N a - \Delta_{DiV} - \Delta_{AC} \tag{5.5}$$

$$Z_{top} = Z_P + \kappa_u a + \Delta_{VSO} + \Delta_{AC} \tag{5.6}$$

for double null

$$Z_{top} = -Z_{bottom} = \kappa_N a + \Delta_{DiV} + \Delta_{AC} \tag{5.7}$$

Δ_{AC} is a clearance gap for access port.

The prohibition region (iii) is also defined by

$$X_{inside} \leq X_{EX} \leq X_{outside} \tag{5.8}$$

$$Z_{EX} \leq -\kappa_N a \tag{5.9}$$

where $$X_{inside} = \sigma_N R_p + \Delta_{Exh} - \Delta_{leg} \tag{6.10}$$

$$X_{outside} = \sigma_N R_p + \Delta_{Exh} + \Delta_{leg} \tag{5.11}$$

Δ_{Exh} is specified as a distance between null point and the center line of exhaust duct, and Δ_{leg} is also specified as a space for exhaust duct and supporting leg. PFC coils are set automatically to avoid these prohibition regions

The divertor coils will be set on the extented line connecting the null point and plasma center.

The cross section of EF coils are given initially. However, as discussed in Sec. 7, they are solved consistently with conductor design constraints and operation scenario.

6. Plasma equilibrium calculations

The free-boundary toroidal MHD equilibrium code "EQUCIR"[15] has been used in this design code to evaluate the currents in the poloidal field coils that maintain given plasma shape and plasma parameters. Plasma shape is defined by a magnetic surface having a 95 % flux. For a desired plasma shape, averaged elongation and triangularity, $\tilde{\kappa}$ and $\tilde{\delta}$, magnetic null points (R_N, Z_N) are given by the following relations,

$$R_N = R_p - \delta_N a \ , \quad Z_N = Z_p \underset{(+)}{-} \kappa_N a \ . \tag{6.1}$$

where

$$\kappa_N = 1.24 \hat{\kappa} - 0.13 \ , \quad \delta_N = 1.52 \hat{\delta} - 0.085 \tag{6.2}$$

$\hat{\kappa} = \tilde{\kappa}$ and $\hat{\delta} = \tilde{\delta}$ for double null configuration, on the other hand $\hat{\kappa} = 1.2\ \tilde{\kappa}$ and $\hat{\delta} = 1.4\ \tilde{\delta}$ for single null configulation. Z_p is a distance between TFC midplane and plasma axis. These relations are based on our experiences on plasma equilibrium studies. If the obtained plasma shape will differ from the desired shape largely, the results will be omitted from a scope. Optimization for the external coil currents and their positioning is not carried out in the code.

The coil currents I_n may be described as a linear function of ψ_p and I_p such as $I_n = C_{1,n}\ \psi_p + (C_{2,n}\ \beta_p + C_{3,n}) I_p$. So, current patterns with ψ_p can be obtained by calculating the coil currents of at least two ψ_p under constant I_p and β_p. We determine the current patterns for two phases, namely burning phase and ramp up phase, as the following form,

$$I_{coil}^{burn}\ (n) = A_n^{burn}\ \psi_p + B_n^{burn} \tag{6.3}$$

$$I_{coil}^{ramp}\ (n) = A_n^{ramp}\ \psi_p + B_n^{ramp} \tag{6.4}$$

7. Operation scenario

7.1 Required volt second

Operation scenario is one of important design driver to determine not only reactor size but also reactor's capability. Considering that there is a variety of operation scenarios to be chosen such as full-inductive operation, non-inductive ramp-up, quasi-steady state operation, heating method, current ramp-up method and so on, it is very tough to select a single operation scenario. In this code, we only consider one aspect of operation scenario, that is, a required volt second. Reactor's capability is not discussed.

As discussed in Section 3.1, a necessary volt second $\Delta\phi$ has to be given initially to determine the inner torus radial-build.

(1) Case of full inductive operation

In this case, we estimate the necessary volt second from Ejima's emperical law, that is,

$$\Delta\phi = \phi_{Ejima} + \phi_{ex} + \phi_{burn} \tag{7.1}$$

$$\phi_{Ejima} = 1.35 \times 10^{-6} R_p I_p \tag{7.2}$$

$$\phi_{ex} = \mu_0 (\ell n\ 8A-2) R_p I_p \tag{7.3}$$

$$\phi_{burn} = 2.092 \times 10^{-3} \frac{Z_{eff}\ t_B}{\kappa a^2 T_e^{1.5}} R_p I_p \tag{7.4}$$

where t_B is burn time. Schematic drawing of full inductive pulsed operation is shown in Fig. 4. There are five phases in an operation, namely, plasma break-down, joule heating, additional heating, burning and shut down. One turn voltage in plasma break-down V_ℓ^{bd} and break-down time $(t_2 - t_1)$ will be specified in typicaly 30 ~ 50 V and 15 m sec, respectively. In joule heating and additional heating phases, current ramp-up speed $\dot{I}_p$ is specified based on experimental data so that one turn voltage in these phases is given by a sum of $L_p \dot{I}_p$ and $R_p I_p$.

(2) Case of none inductive current ramp up

In this scenario, plasma current is raised by RF or NBI current drive and OH flux is consumed mainly in burning phase. Hence, a necessary volt·

second $\Delta\phi$ is given as

$$\Delta\phi = \phi_{ign} + \phi_{burn} \tag{7.5}$$

where ϕ_{ign} is a required flux during ignition approach phase, Fig. 5 shows a schematic drawing of this operation. If OH assist during plasma break down is accounted, the additional volt second will be required.

7.2 Consistency of PFC system

Initial determination of the reactor size greatly depends on the value f_{EQ} in Eq. (3.1). Being strict about the volt second required from the operation scenario, the end radius of the solenoid coils will be adjusted consistently with conductor design constraints. From equilibrium calculations, patterns of the PFC coil currents are obtained. The maximum current at the solenoid coils is limited from allowable maximum magnetic field. The field calculations with current PFC configulation is carried out in the code and the magnetic flux at the swing end, $\psi_p^{\text{swing end}}$, is found by constraint of maximum field at the solenoid coils. Then the magnetic flux at the start of burning, $\psi_p^{\text{burn start}}$ is obtained by $\psi_p^{\text{burn start}} = \psi_p^{\text{swing end}} + \phi_{burn}$. By similar process following operation scenario, $\psi_p^{\text{swing start}}$ is obtained retroactively. Magnetic field at the solenoid coils is reexamined at each ψ_p. If the available flux swing, $\Delta\phi^{av} \equiv |\psi_p^{\text{swing start}} - \psi_p^{\text{swing end}}|$, satisfies the required volt second $\Delta\phi$, there is no further chage of the radial-build. However, if $\Delta\phi^{av}$ is too small or too large compared with $\Delta\phi$, either f_{EQ} or bore of solenoid coils is adjusted and full calculations are done again. If $\Delta\phi^{av} \simeq \Delta\phi$, but the maximum field generated at the other EF coils exceed the maximum field constraints, the cross sectional area of the coils will be changed and equilibrium calculations are repeated. In these processes, PFC system is designed consistently with the operation scenario.

7.3 Consistency of TFC design

After PFC system and their currents pattern are fixed, actual overturning force on the toroidal coils are evaluated with field calculations. If the actual poloidal magnetic field normal to the current direction of TFC, B_{pn}^{act}, would exceed greately over the initial B_{pn}^{int}, the side plate thickness of TFC case may not be enough for bending

and tensile stress against the overturing force. In this case, the thickness of the side plate and the space factor f_{ts} of TFC can be changed for the recalculation of radial-build.

8. Electric power supply estimations

The major part of the magnetic field should be supplied from the SC coils. The accumulated capacity of the poloidal field coil power supplies is dominant to compare with that of the toroidal field coil power supplies. Hence, the system study may be concentrated to the former.

8.1 Poloidal field coil power supply

The poloidal field system has many coils and these coils have mutual coupling. The power demand in the ramp-up phase is larger than that in the burn phase. Hence, it may be assumed that the poloidal field energy is stored in the flywheels and the power is supplied through the motor-generator system.

To evaluate the capacity, it is necessary to estimate the required voltage for each coil. Then, considering the circuit configuration, the required power from each coil is calculated.

(1) Terminal voltage of PF coils

To evaluate the required voltage from each coil, its current I(t) and the mutual inductance M(i,j) are prepared from the poloidal field design. Plasma current is assumed to be one turn coil.

The coil voltage for the j-th coil E_{dj} is given by,

$$E_{dj} = \sum M_{jk} \Delta I_k/\Delta t + R_j I_j \qquad (8.1)$$

where R_j is the resistance component. $\Delta I_k/\Delta t$ is determined by the operation scenario.

Probably the required voltage is high enough in the first break down phase. Hence, DC power supply voltage may strongly depend on this voltage generation circuit

(2) DC power supply

A DC power supply is composed of the two parts, i.e., convertor and transformer. To evaluate its voltage, it is necessary to consider the circuit configuration, i.e., a first commutating switch is applied or not, and a convertor is conventional, bidirectional or a mixed type.

1) Convertor

The capacity of the j-th coil P_j is given by

$$P_j = E_{dj\ max} \cdot I_{j\ max}(1 + \delta) \tag{8.2}$$

where suffix "max" means the maximum value. δ is the circulating current factor which is evaluated to be 0.1 ~ 0.15 in the bi-directional type and replaced with zero in the conventional type.

2) Transformer

The capacity of the j-th power supply U_j is given by

$$U_j = \sqrt{2} \cdot E_{sj} \cdot I_{j\ max}(1 + \delta) \tag{8.3}$$

with

$$E_{sj} = \frac{E_{dj\ max}}{K_1\left(K_2 \cos\alpha_{min} - \frac{IX}{2} - \frac{\pi}{3} \cdot IR\right)} \tag{8.4}$$

where

K_1 conversion factor (1.39: 12 phase rectifier)

K_2 voltage fluctuated factor (0.9)

α_{max} minimum controled phase (~20°)

IX reactance component (~0.1)

IR resistive component (~0.05)

Here, the value in the brackets is a typical value.

When the required current is I_j, the apparent power is given by

$$U_j^1 = U_j \frac{I_j + \delta I_{j\ max}}{I_{j\ max}(1 + \delta)} \tag{8.5}$$

3) System capacity

It is necessary to consider the positive component and negative component in the bi-directional type. Hence the accumualted convertor capacity P is

$$P = \sum P_{j\oplus} + \sum P_{j\ominus} \tag{8.6}$$

and the transformer capacity U is

$$U = \sum U_{j\oplus} + \sum U_{j\ominus} \tag{8.7}$$

where suffix $\oplus$ or $\ominus$ means the positive or the negative component.

The effective power of the jth coil is evaluated by $p_j = E_{dj} \cdot I_j$ and there required energy is given

$$E_j = \int_{-T_p}^{T} p_j \, dt \tag{8.8}$$

where T_p is precharging time and T is operation time. The flywheel capacity E is assumed to be

$$E = \sum E_j \tag{8.9}$$

8.2 Toroidal field coil power supply

The toroidal coil may be charged slow enough (~hours). Hence the required voltage is several tens volts per coil and the power may be several MW. This power is supplied from utility line.

The capacity of power supply P_T is evaluated to be

$$P_T = E_T/\tau \tag{8.10}$$

where E_T is the stored energy and τ is the charging time for the energy.

8.3 Heating and current drive

The system efficiency η is supposed to be given by

$$\eta = \eta_2 \, \eta_3 \, \eta_4 \, / \, (1 + \eta_5)$$

where

η_2 coupling efficiency

η_3 power transfer efficiency

η_4 conversion efficiency from DC power to RF or NB (incl. neutralization etc.)

η_5 input power correction factor

The required power for heating or current drive P is given from the plasma design. Then, the RF or NB source capacity P_o can be expressed as,

$$P_o = P/\eta_2 \, \eta_3 \, \eta_4$$

and input power P_i is estimated by

$$P_i = P(1 + \eta_5) \, / \, \eta_2 \, \eta_3 \, \eta_4 \, .$$

9. Cost estimations

The cost estimation is carried out in the form of relative cost comparison. This is useful to show the cost tendancy due to the design change, especially in the early design stage.

A simple equation shown below is sufficient to estimate the relative cost among the studied machine types. The equation is

$$C = \sum Cri * \left(\frac{Ai}{Ari}\right)^{Ni} \tag{9.1}$$

where Cri, Ari, Ai, and Ni are the cost fraction of the ith item of the reference, the index of the ith item of the reference, that of a sample, and the value chosen from 0.5 to 1.0 suitable to each component, respectively.

It is important to select components, the costs of which behave independently of each other to the given conditions. The index representing the component should be flexible enough to respond to the change through the design progress. The developed system integration, and its typical indexes of two kinds each are summarized in Table 1.

The cost fraction for each component should be arranged initically as the reference. The indexes are able to be selected corresponding to the design condition at the time.

10. Example of results

We show a set of results for an example reactor. Major system quantities are obtained in the code, such as plasma parameters, geometrical parameters, toroidal and poloidal field coil system quarities, required heating power, and so on. In addition, figures of major system quantities are available. Here, we show these figures. Figure 6 ~ 17 show the radial build, vertical build, inplane structure, total ampere-turn of poloidal field coil system as a function of supplied flux ψ to the plasma, current pattern of each poloidal field coil at ψ = -20 V·S, poloidal field coil current as a function of flux at high beta, equi-heating power contour in n-T plane to obtain the required heating power, inplane force pattern on TF coils, over-turning force pattern on TF coils at the time of start of burn, plasma equilibrium configuration at high beta, and field pattern of external field coils, respectively.

Acknowledgement

Authors are grateful to Drs. S. Tamura, M. Yoshikawa and K. Tomabechi for their continuous encouragement throughout this work.

10. Example of results

We show a set of results for an example reactor. Major system quantities are obtained in the code, such as plasma parameters, geometrical parameters, toroidal and poloidal field coil system quarities, required heating power, and so on. In addition, figures of major system quantities are available. Here, we show these figures. Figure 6 ∿ 17 show the radial build, vertical build, inplane structure, total ampere-turn of poloidal field coil system as a function of supplied flux ψ to the plasma, current pattern of each poloidal field coil at ψ = -20 V·S, poloidal field coil current as a function of flux at high beta, equi-heating power contour in n-T plane to obtain the required heating power, inplane force pattern on TF coils, over-turning force pattern on TF coils at the time of start of burn, plasma equilibrium configuration at high beta, and field pattern of external field coils, respectively.

Acknowledgement

Authors are grateful to Drs. S. Tamura, M. Yoshikawa and K. Tomabechi for their continuous encouragement throughout this work.

References

(1) J.C.Deboo, et al., Nuclear Fusion, 26 (1986) 211
(2) Y.Shimomura et al., JAERI-M 87-080 (1987).
(3) INTOR, Phase One, IAEA, Vienna (1982)
(4) W.Pfeiffer, et al., Nuclear Fusion, 19 (1979) 51
(5) M.Keilhacker, et al., 4th Intn'l Symp. on Heating in Toroidal plasmas, Rome, March (1984)
NET Status Report, NET Team, Decmber (1985)
(6) INTOR, Phase Two A, Part 1, IAEA, Vienna (1983)
V.M.Leonov, et al., Plasma Physics and Controlled Nuclear Fusion Research, IAEA, Vienna (1980) 393
(7) R.J.Goldston, Plasma Physics and Controlled Fusion, 26 (1984) 87
(8) F.Troyon, et al., Plasma Physics and Controlled Fusion, 26 (1984) 209
(9) T.Tuda, et al., Plasma Physics and Controlled Fusion, 26 (1984)
(10) L.C.Bernard, et al., Nuclear Fusion, 23 (1983) 1475
(11) K.Yamasaki, etal., Nuclear Fusion, 25 (1985) 1543
(12) M.Sugihara, et al., J. of Nucl. Sci. and Tech., 19 (1982) 608
(13) D.L.Jassby, MATT - 1074, (1974)
(14) D.R. Mikkelsen, et al., PPPL - 1929 (1982)
(15) H.Ninomiya, et al., JAERI-M 9127 (1980)
K.Shinya, et al., JAERI-M 9278 (1981)
(16) R.J.Thome and J.M.Tarrh, MHD and Fusion Magnets, John Willy & Sons (1982)

Table 1 System Integration and Indexes

NO.	COMPONENTS	Cri (%)	INDEX A 1	2
1	REACTOR STRUCTURE	16	RakVALUE	WEIGHT
2	TF COIL	13	ENERGY	AT.km
3	PF COIL	9	ENERGY	AT.km
4	COIL SUPPORT	3	ENERGY	WEIGHT
5	REACTOR ASSEMBLY	8	WEIGHT	COMPLEXITY
6	TRITIUM/FUEL/ PUMPING SYSTEM	4	FUSION OUTPUT	QUANTITY
7	MAINTENANCE/ REPAIRING SYSTEM	3	WEIGHT	COMPLEXITY
8	COOLING SYSTEM	2	HEAT LOAD	QUANTITY
9	REFRIGERATION SYSTEM	4	HEAT LOAD	QUANTITY
10	HEATING/CURRENT DRIVE SYSTEM	16	POWER	QUANTITY
11	TF COIL P.S.	1	ENERGY	CAPACITY
12	PF COIL P.S.	5	ENERGY	CAPACITY
13	HEATING P.S.	1	POWER	QUANTITY
14	INSTRUMENTATION/ CONTROL SYSTEM	6	—	—
15	BUILDINGS/ FACILITIES	9	AREA	CAPACITY
	(TOTAL)	100		

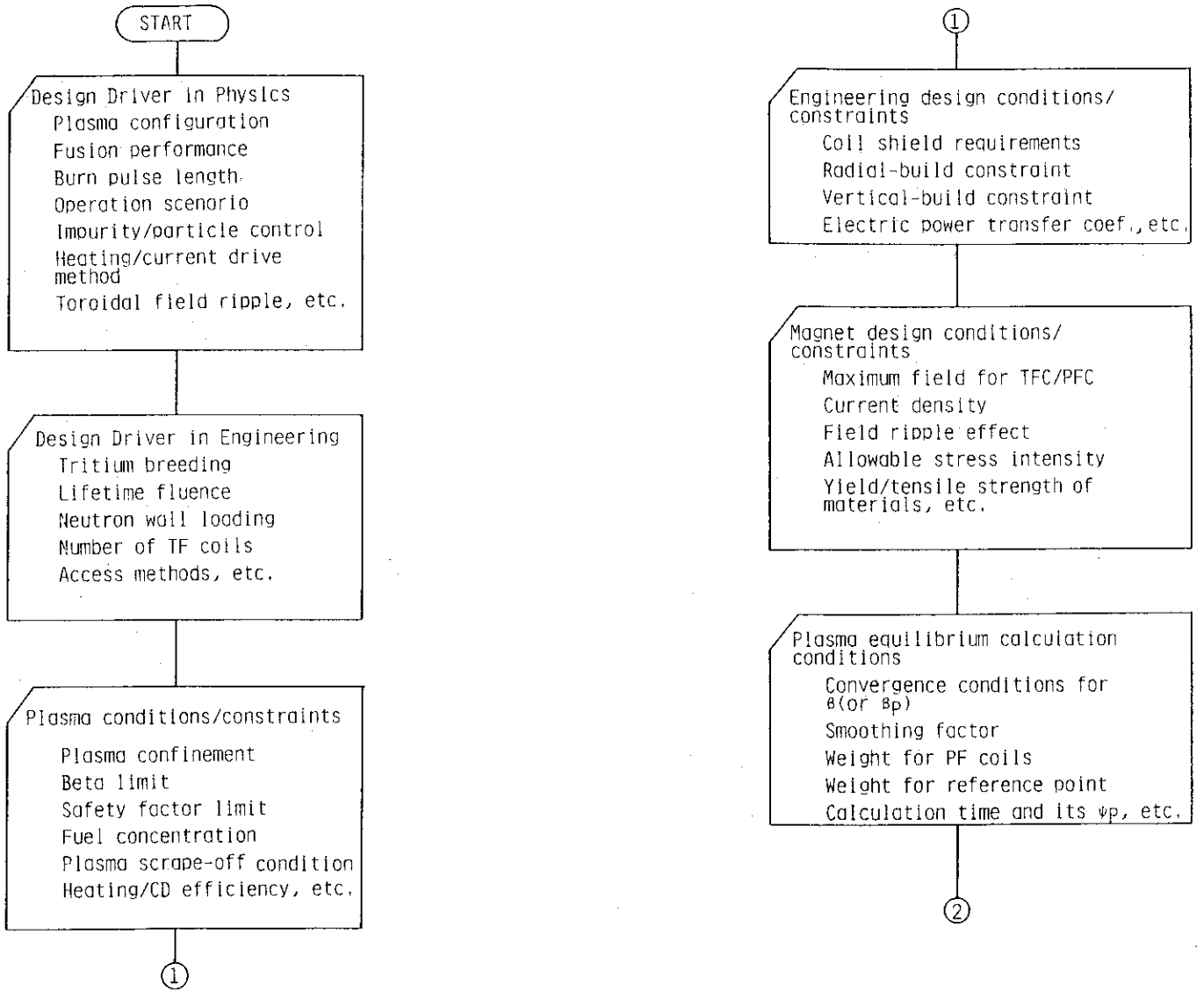

Fig. 1 Flow chart of TRESCODE
(Tokamak REactor System COnceptual DEsign code)

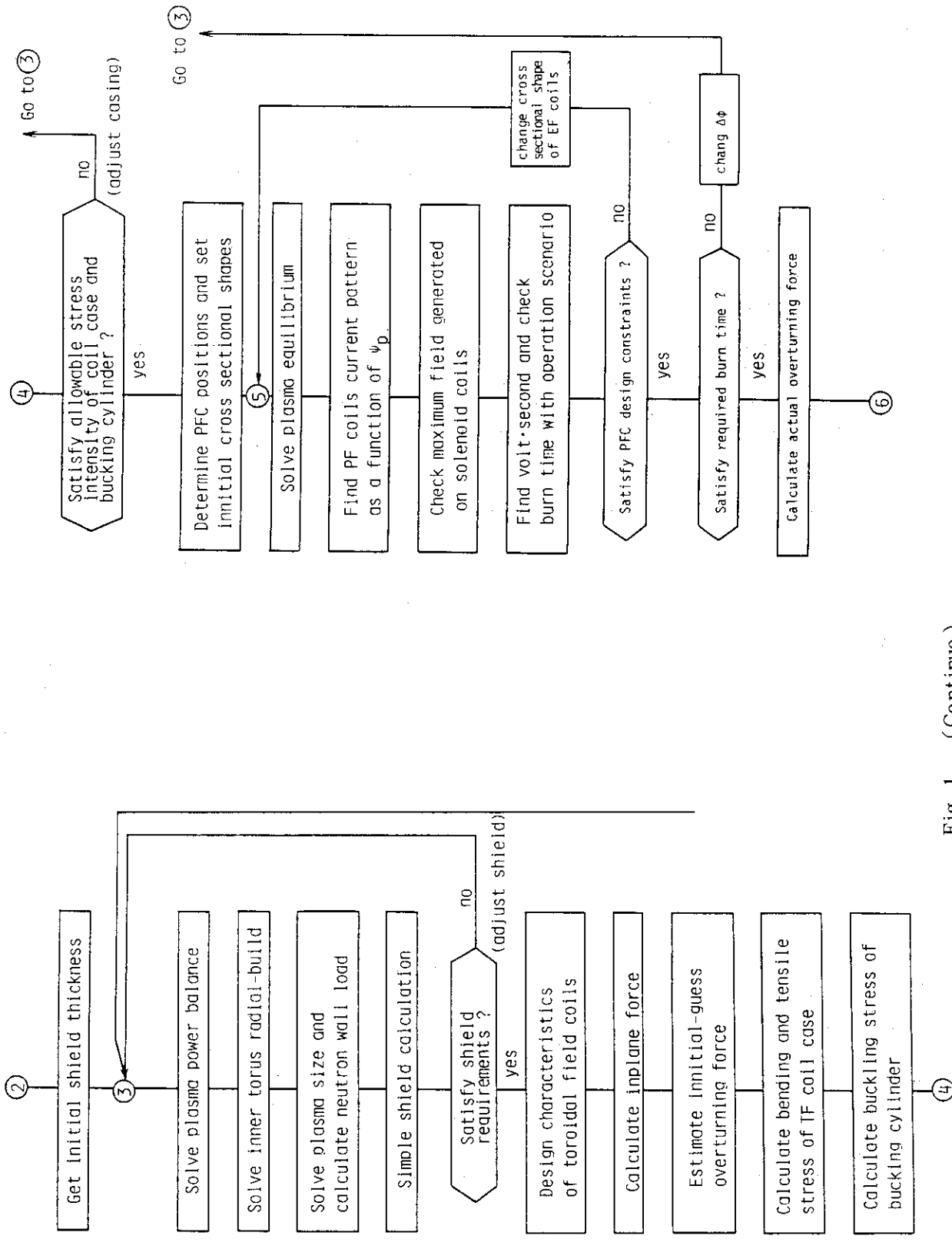

Fig. 1 (Continue)

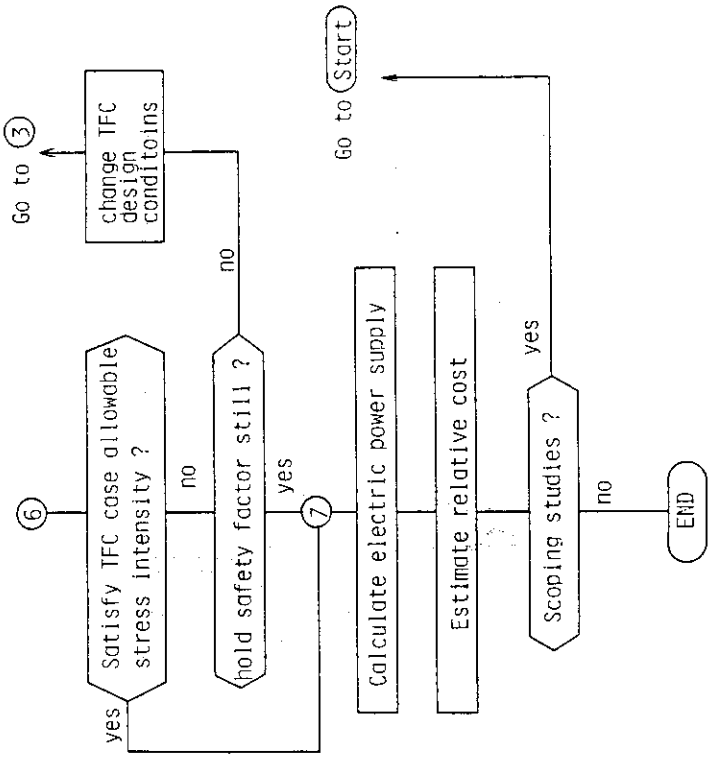

Fig. 1 (Continue)

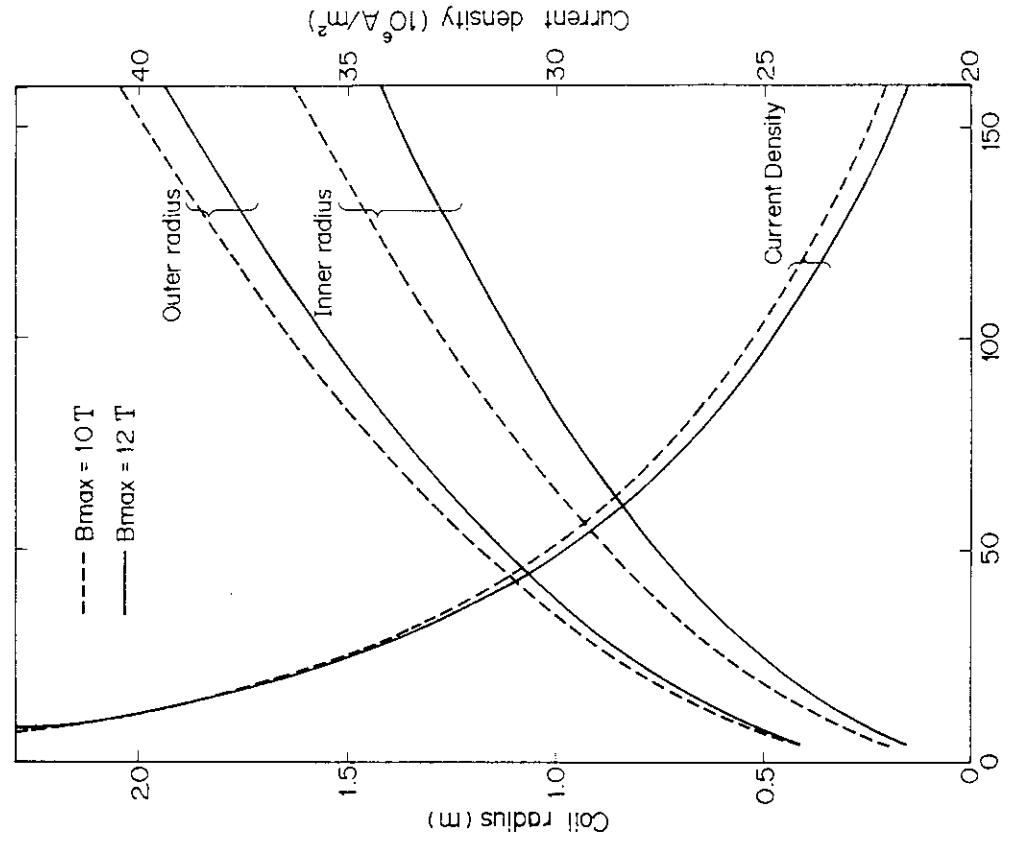

Fig. 3 OH coil radius and current density

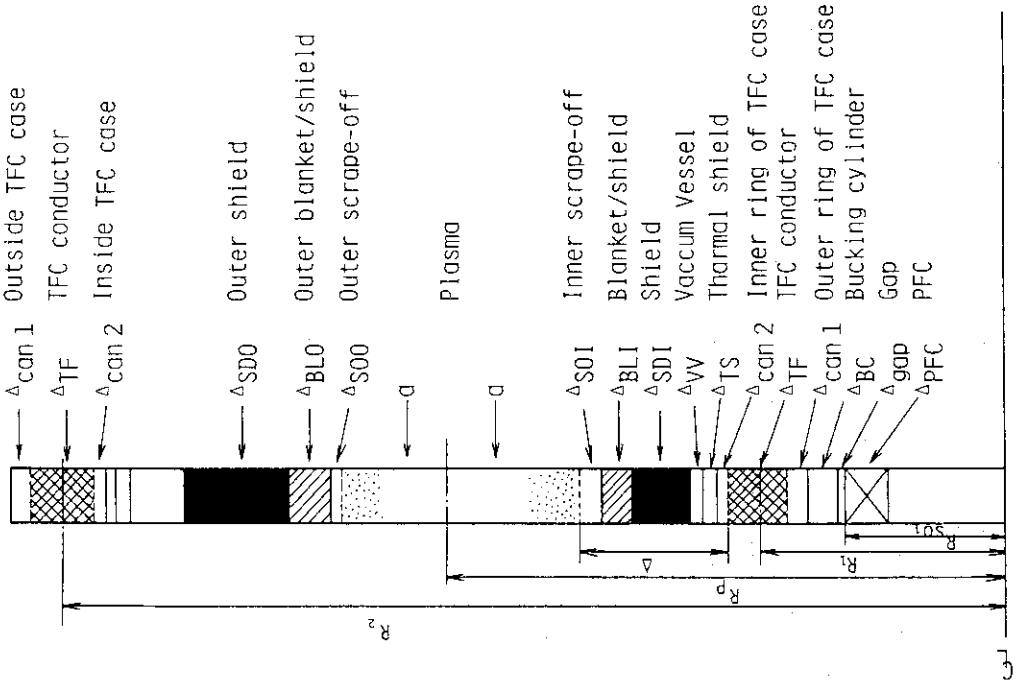

Fig. 2 Radial-build

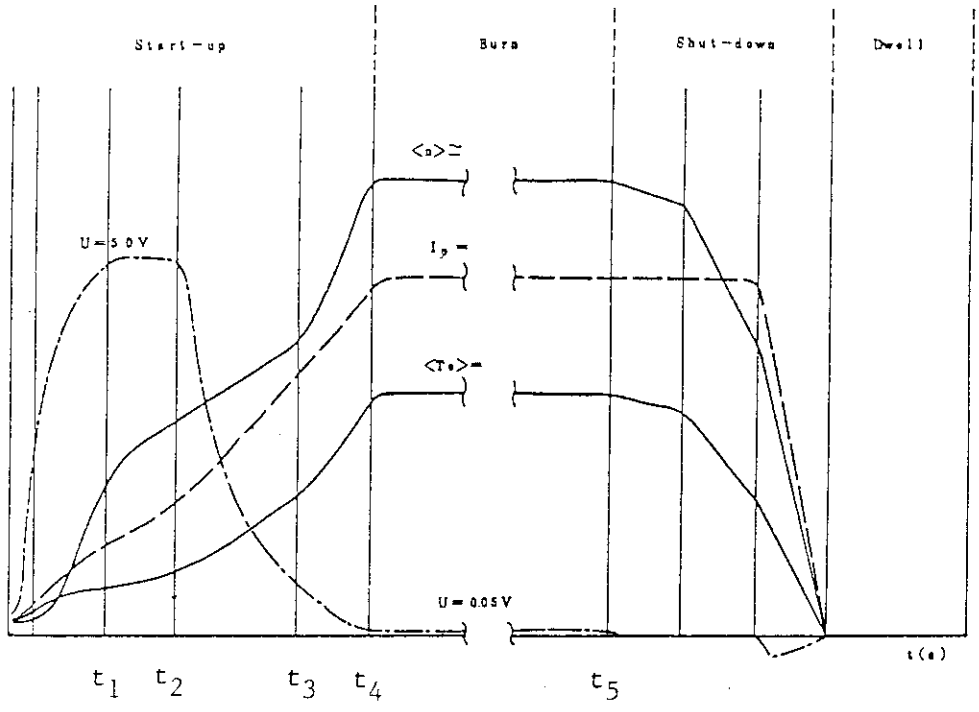

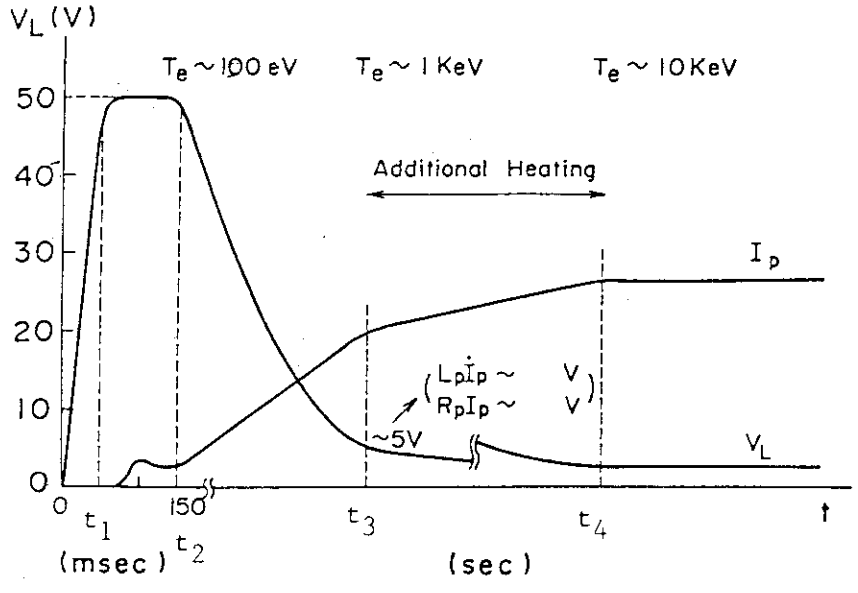

Fig. 4 Full Inductive Operation Scenario

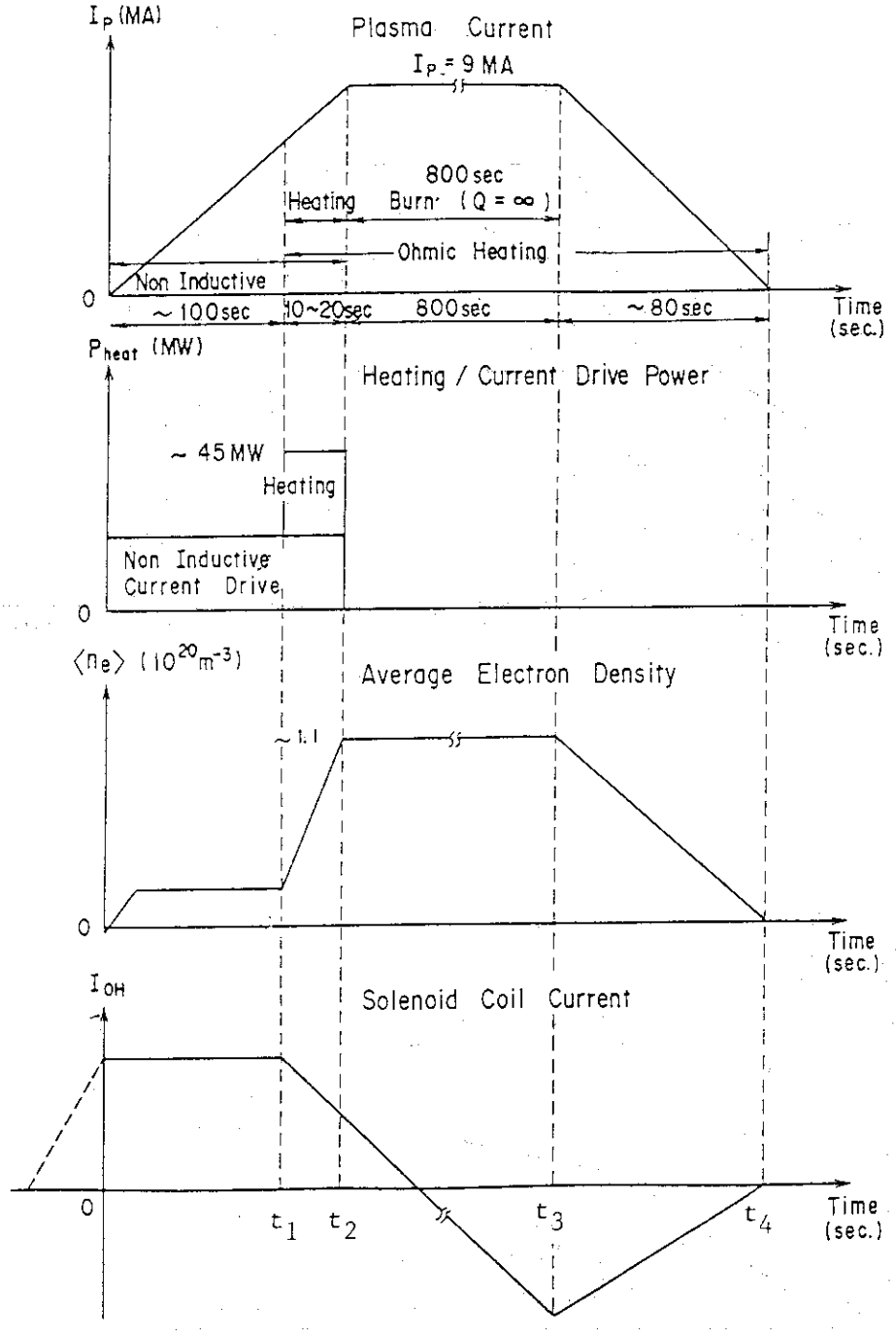

Fig. 5 Non-inductive Current Ramp up Operation Scenario

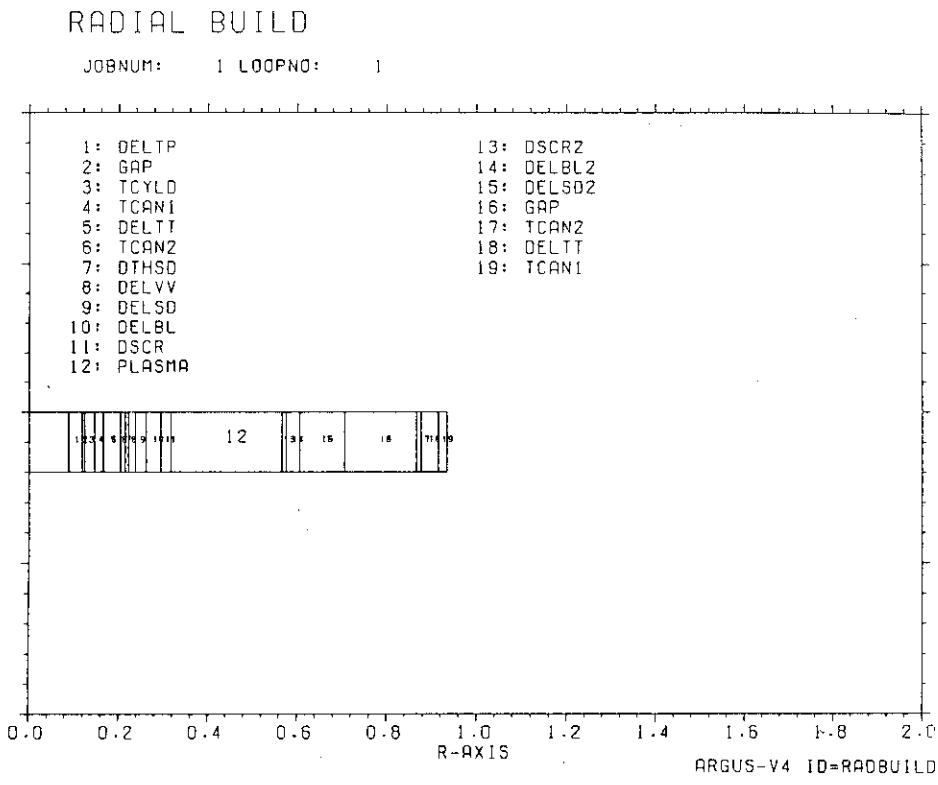

Fig. 6 Radial build

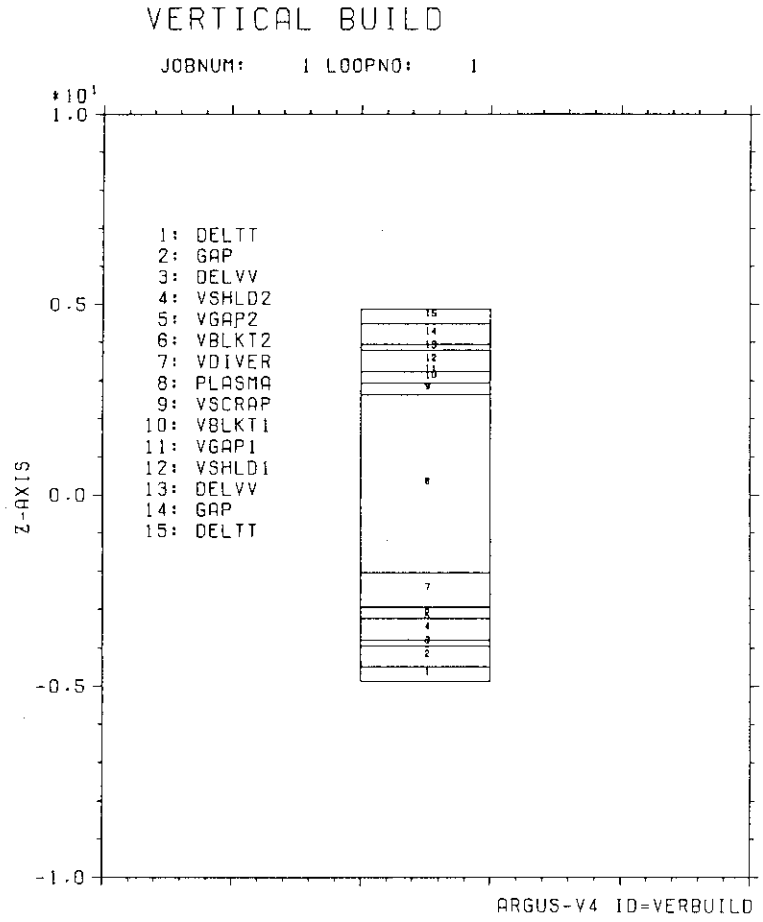

Fig. 7 Vertical build

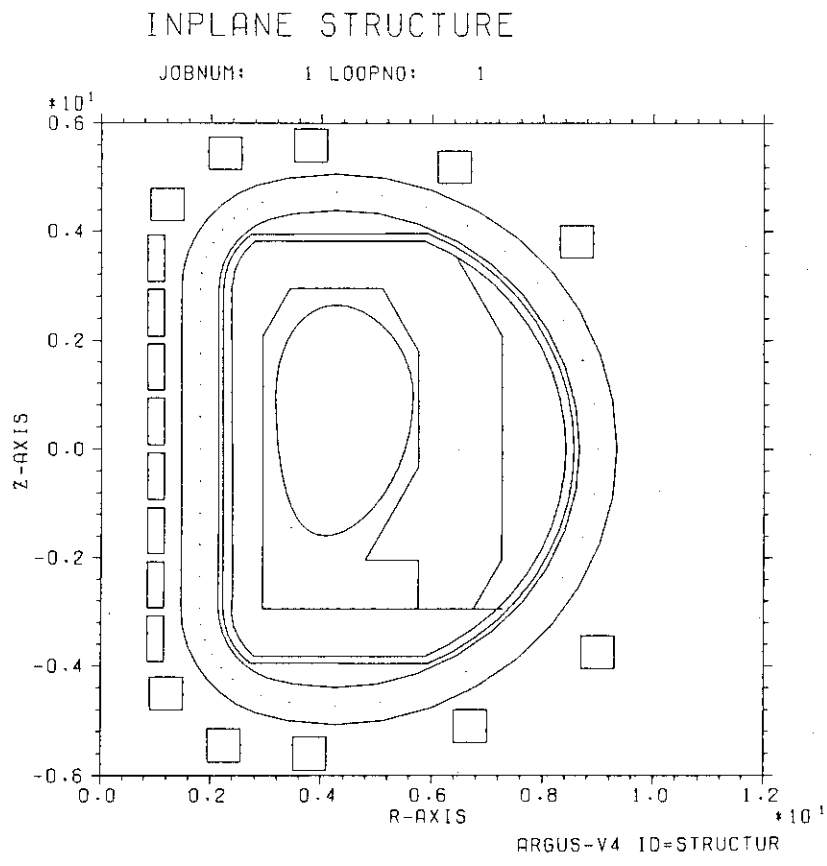

Fig. 8 Inplane structure

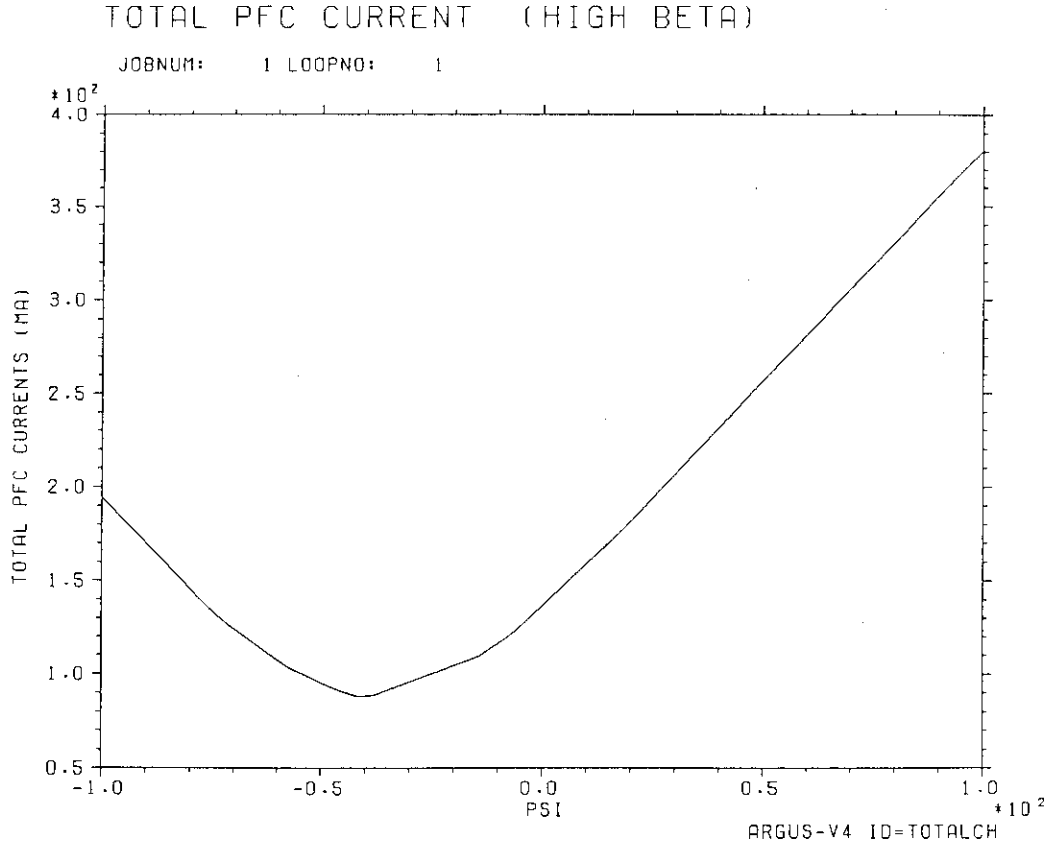

Fig. 9 Total PFC current as a function of ψ

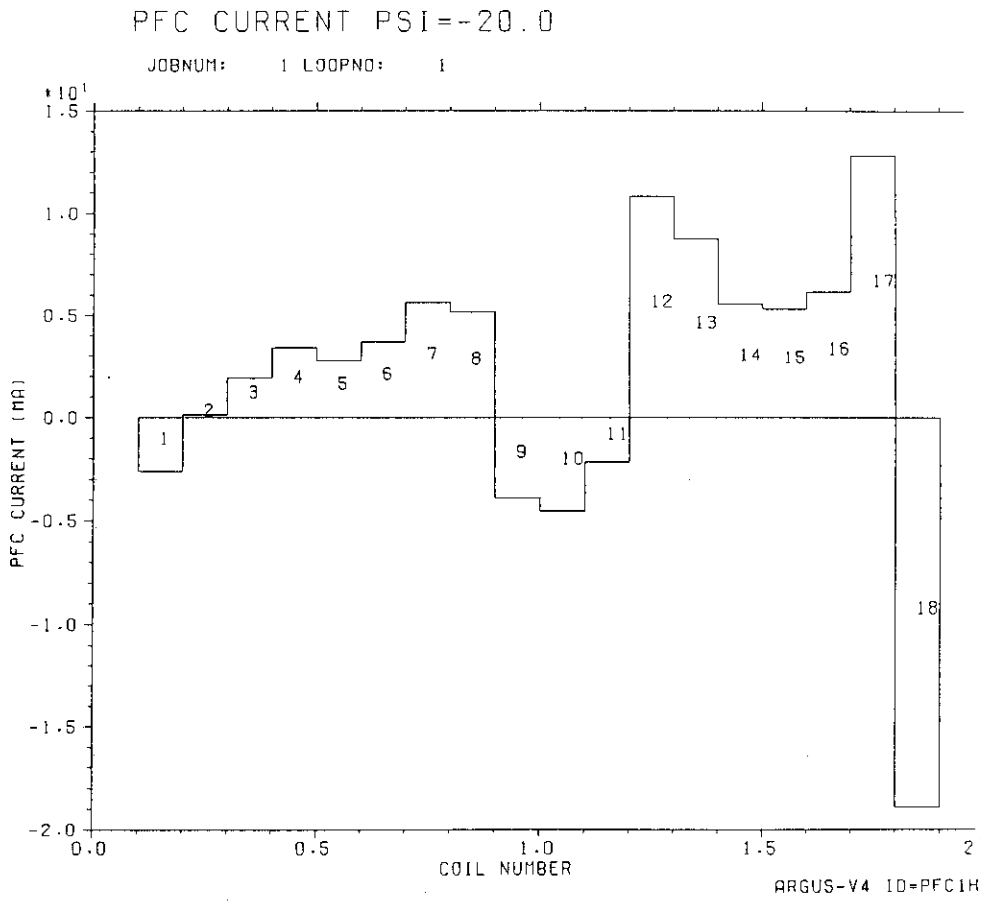

Fig. 10 PFC current putern of
$\psi = -20$ V. S

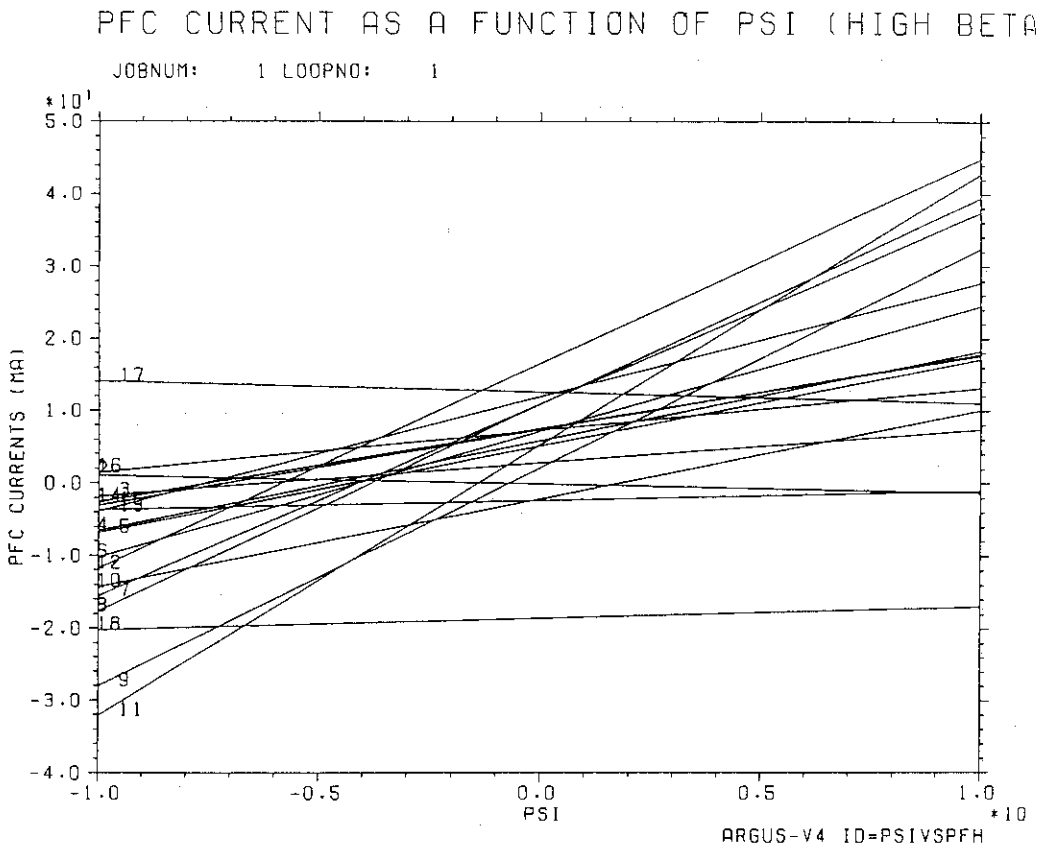

Fig. 11 PFC current as a function of ψ for high beta plasma

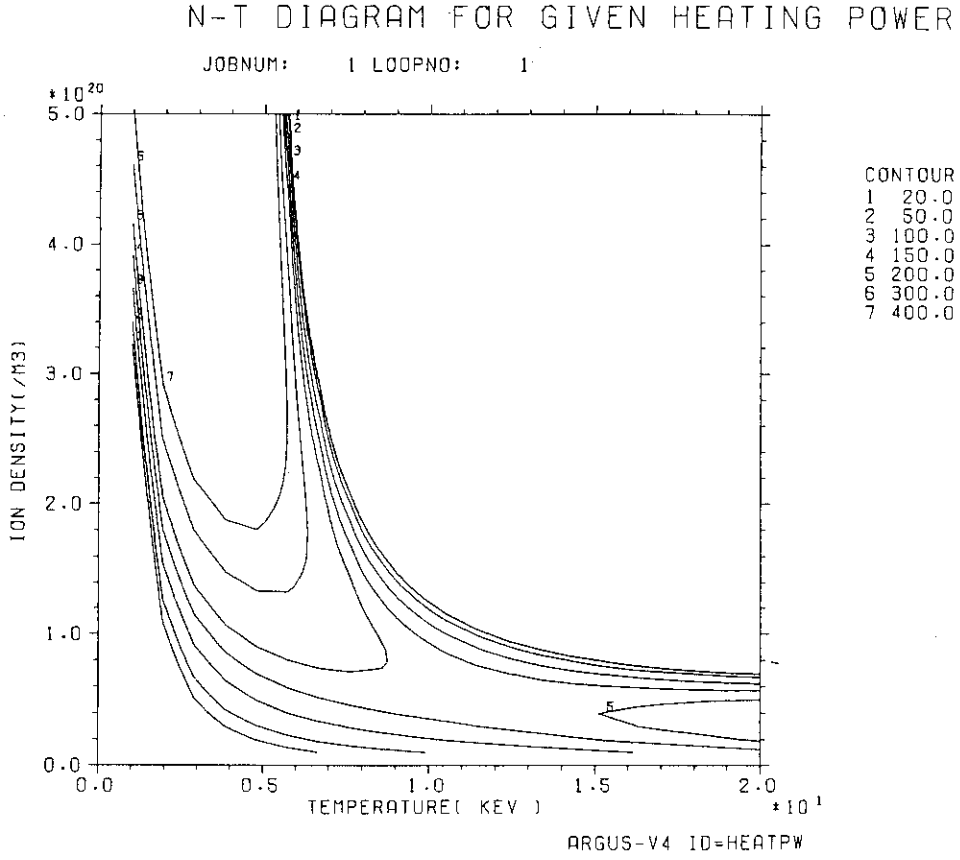

Fig. 12 Equi-heating pourer contour in n-T plane

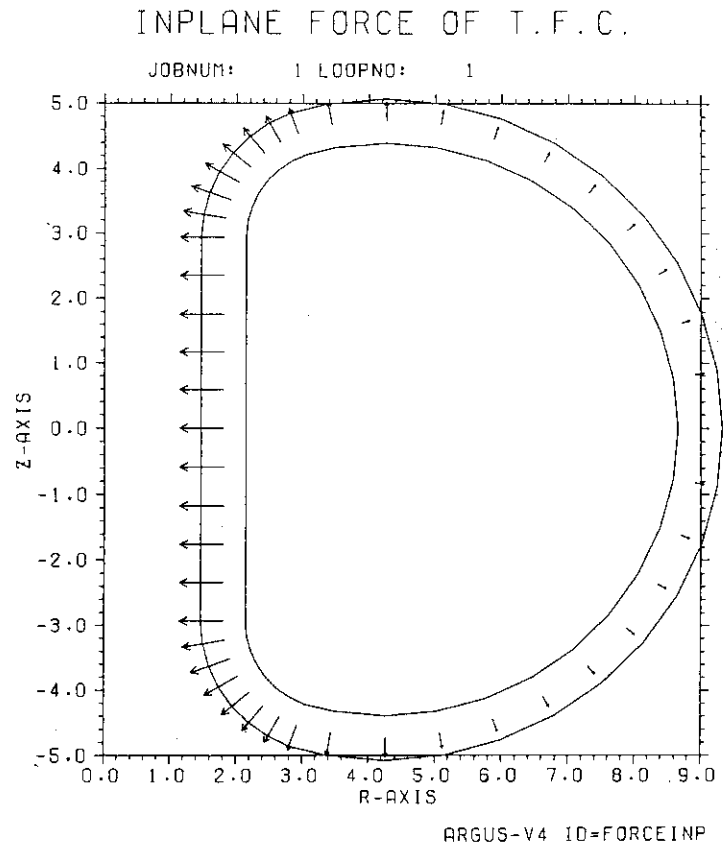

Fig. 13 Inplane force of Troidal field coils

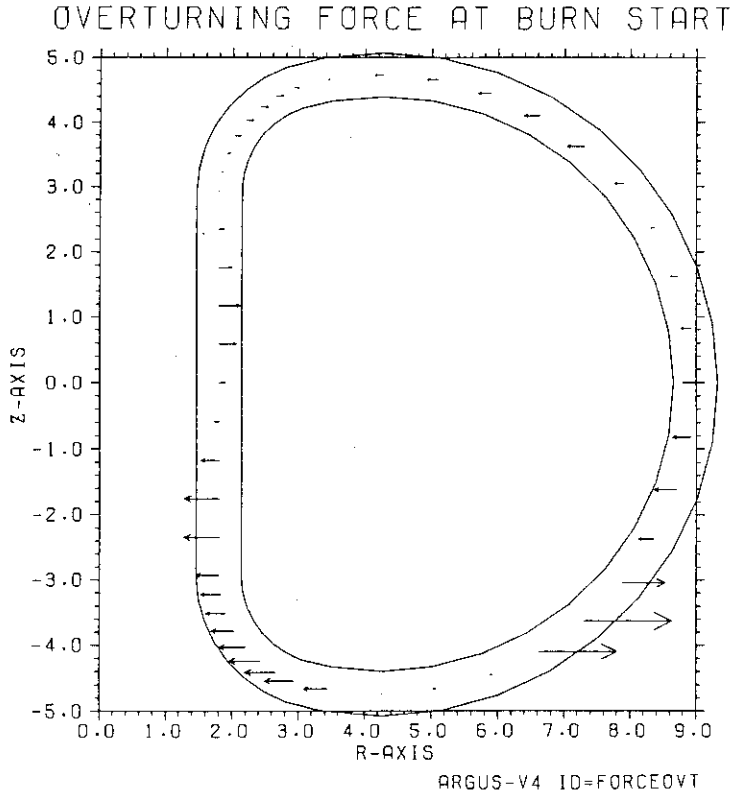

Fig. 14 Ouer−turning force TF coils at bnrn start

FER61 OPTION ACS PLASMA (MIRNOV,TROYON)
TEST RUN OF TRESCODE ON 87/4/21

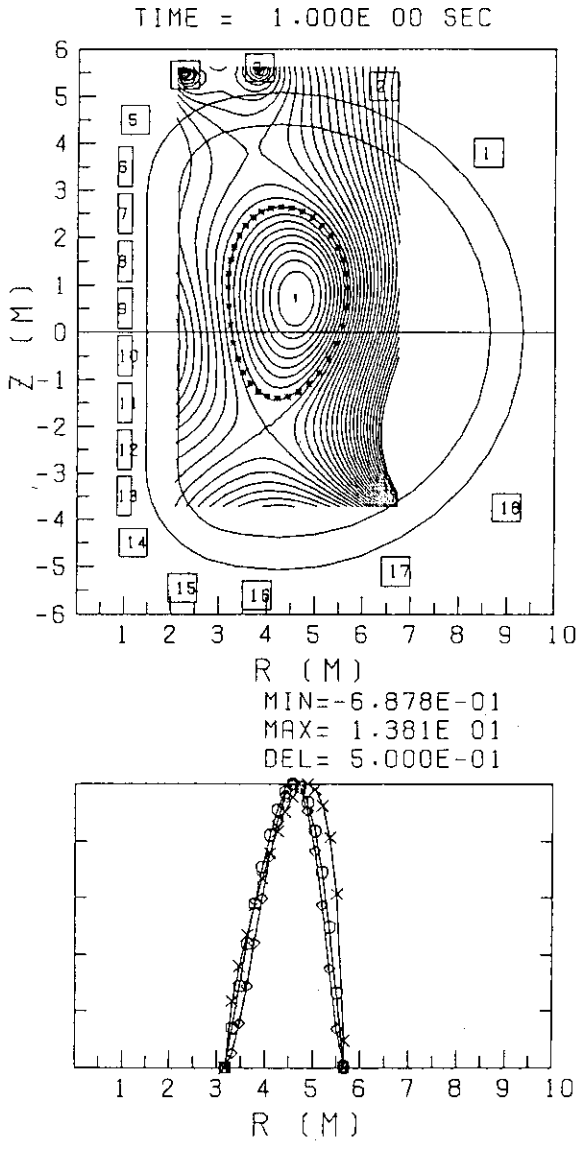

***** PLASMA PARAMETERS *********

IP-CURRENT	(A)	8.703E 06
VLOOP-SURFACE	(V)	-5.851E 01
SELF INDUCTANCE	(H)	8.551E-06
SMALL LI		8.601E-01
R-AVERAGE	(M)	4.419E 00
R-INNER	(M)	3.178E 00
R-OUTER	(M)	5.660E 00
R-MAGNETIC AXIS	(M)	4.601E 00
R-CURRENT MAX.	(M)	4.858E 00
A-HALF WIDTH	(M)	1.241E 00
A-AVERAGE	(M)	1.620E 00
ELLIPTICITY		1.705E 00
CROSS AREA	(M**2)	8.245E 00
VOLUME	(M**3)	2.258E 02
TOROLDAL BETA	(MHD)	5.293E-02
POLOIDAL BETA	(MHD)	1.863E 00
POLOIDAL BETA	(AREA)	1.226E 00
POLOIDAL BETA	(VOLUME)	1.260E 00
Q-VALUE	(MHD)	3.633E 00
BV-SHAFRANOV	(T)	-6.204E-01
BV-CALCULATED	(T)	-5.734E-01
SUPPLIED FLUX	(WB)	1.179E-04
ABS TOTAL AMP	(AT)	1.366E 08
STORED ENERGY	(J)	8.902E 09
AMP-T METER	(AT-M)	2.655E 09
LIMITER R	(M)	3.993E 00
Z	(M)	-2.039E 00
PSI	(WB)	9.312E 00
RP (95%)	(M)	4.430E 00
AP (95%)	(M)	1.199E 00
ZP (95%)	(M)	7.210E-01
ELON-UPPER	(95%)	1.543E 00
ELON-LOWER	(95%)	1.978E 00
TRIANG-UPPER	(95%)	1.439E-01
TRIANG-LOWER	(95%)	2.737E-01

Fig. 15 Equilibrium configuration of plasma

FER61 OPTION ACS PLASMA (MIRNOV,TROYON)
TEST RUN OF TRESCODE ON 87/4/21

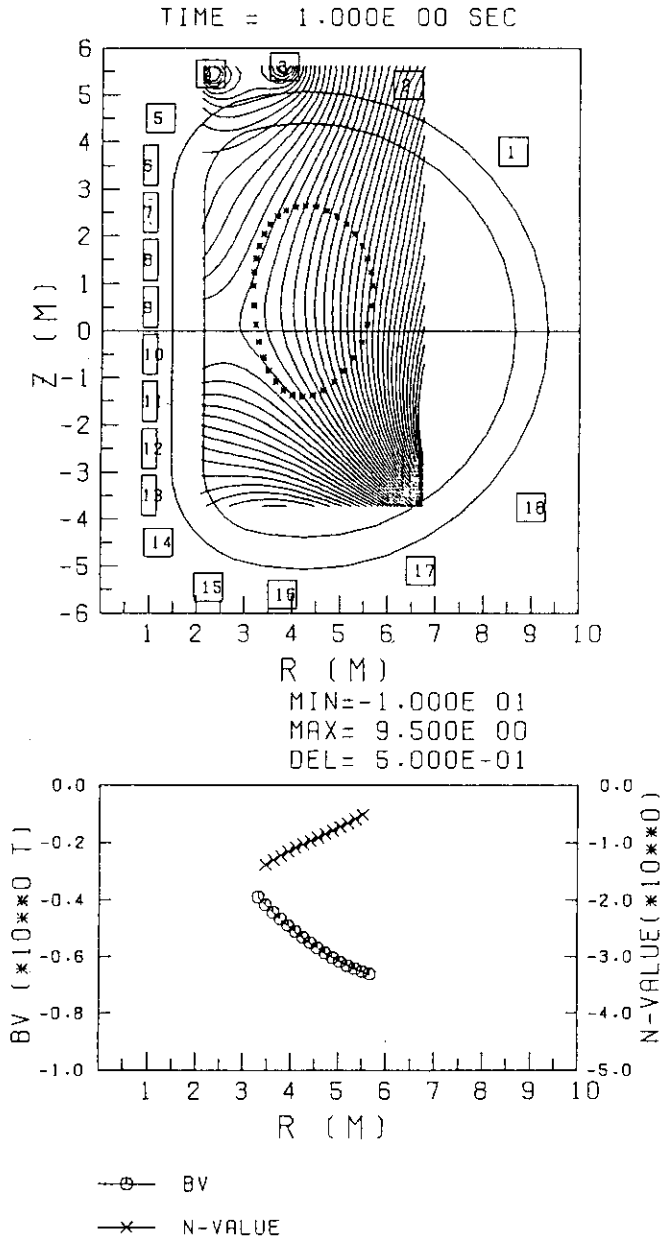

***** COILS **********

NO.	CURRENT(A)	BV(T)
1	-2.340E 06	-1.521E-01
2	-8.151E 04	-3.385E-03
3	2.832E 06	4.049E-02
4	5.875E 06	2.506E-02
5	5.143E 06	3.616E-03
6	7.155E 06	-2.273E-03
7	1.092E 07	-1.944E-02
8	1.088E 07	-3.708E-02
9	2.163E 06	-8.207E-03
10	-2.100E 06	5.267E-03
11	5.328E 06	-4.521E-03
12	1.651E 07	3.544E-03
13	1.191E 07	7.863E-03
14	7.556E 06	8.314E-03
15	7.400E 06	2.724E-02
16	7.312E 06	7.540E-02
17	1.254E 07	3.722E-01
18	-1.859E 07	-8.920E-01

Fig. 16 Equilibrium magnetic field